HOSTED BY

ELSEVIER

Available online at www.sciencedirect.com

ScienceDirect

Journal of Magnesium and Alloys 4 (2016) 151–172
www.elsevier.com/journals/journal-of-magnesium-and-alloys/2213-9567

Review

A review on hot tearing of magnesium alloys

Jiangfeng Song [a], Fusheng Pan [a,b,*], Bin Jiang [a,b], Andrej Atrens [c], Ming-Xing Zhang [c], Yun Lu [d]

[a] National Engineering Research Center for Magnesium Alloys, Chongqing University, Chongqing 400044, China
[b] Advanced Materials Research Center, Chongqing Academy of Science & Technology, Chongqing 401123, China
[c] School of Mechanical and Mining Engineering, The University of Queensland, St. Lucia, QLD 4072, Australia
[d] Graduate School & Faculty of Engineering, Chiba University, 1-33, Yayoi-cho, Inage-ku, Chiba, 263-8522, Japan

Received 27 July 2016; revised 24 August 2016; accepted 24 August 2016

Available online 31 August 2016

Abstract

Hot tearing is often a major casting defect in magnesium alloys and has a significant impact on the quality of their casting products. Hot tearing of magnesium alloys is a complex solidification phenomenon which is still not fully understood, it is of great importance to investigate the hot tearing behaviour of magnesium alloys. This review attempts to summarize the investigations on hot tearing of magnesium alloys over the past decades. The hot tearing criteria including recently developed Kou's criterion are summarized and compared. The numeric simulation and assessing methods of hot tearing, factors influencing hot tearing, and hot tearing susceptibility (HTS) of magnesium alloys are discussed.

Keywords: Hot tearing; Magnesium alloys; Hot tearing criterion; Numeric simulation; Experimental apparatus; Hot tearing susceptibility

1. Introduction

In comparison with Al alloys and steels, Mg alloys have attracted increasing interest in industrial applications, due to their high specific strength and excellent functional performances [1,2]. At present, the majority of Mg alloys are prepared by conventional casting processes [3,4], defect free castings are highly desirable for the subsequent processing and service. Hot tearing is known as one of the most fatal solidification defects commonly encountered during casting practice [5]. Hence, the resistance to hot tearing of Mg alloys must be an important casting characteristic to be investigated.

Hot tear is different from cold crack since it occurs above the solidus temperature [6]. Hot tearing occurs due to the lack of feeding when stresses exceed the strength of the partially solidified metal [7,8]. In other words, hot tearing is associated with feeding, generated or induced stresses, and developed strength in the mushy zone. Industrial and fundamental studies of this phenomenon show that hot tears initiate when the liquid flow through the mushy zone becomes insufficient to fill initiated cavities [9]. The solid fraction at this stage is close to one [10]. The stresses generally arise from restriction of solidification shrinkage and thermal contraction. Besides, the stresses are concentrated at the hot spots where the casting solidifies last or at areas with sudden changes of cross section [11]. Thus, hot tearing is prone to occur at the hot spot. The mechanical properties (strength and ductility) of the semi-solid alloy can be experimentally determined and are found to be temperature dependent [9].

This review summarizes the hot tearing criteria, simulation models, and experimental set-ups developed to characterize the hot tearing susceptibility (HTS) in the past decades. Eskin et al. [9] reviewed the hot tearing criteria, experimental set-ups of Al alloys. The present review mainly focuses on the hot tearing criteria, experimental set-ups used in Mg alloys. Recently developed hot tearing criteria and new technique used in hot tearing assessment are also included in this review. Besides, the factors influencing hot tearing and the HTS of various Mg alloys are also summarized.

2. Hot tearing criterion

Many theories and criteria are proposed to predict the occurrence of hot tearing. These hot tearing criteria, as reviewed by Eskin [9,12], can be briefly divided into two categories: mechanical and non-mechanical. The mechanical criteria are derived mainly from the mechanical behaviour of semi-solid

* Corresponding author. National Engineering Research Center for Magnesium Alloys, Chongqing University, Chongqing 400044, China. Fax: +86 023 65112635.
E-mail address: fspan@cqu.edu.cn (F. Pan).

http://dx.doi.org/10.1016/j.jma.2016.08.003

metals, such as stress, strain, and strain rate. The non-mechanical criteria normally deal with the vulnerable temperature range, phase diagram, and process parameters such as pouring temperature and mould temperature.

2.1. Mechanical based criteria

2.1.1. Critical stress based criterion

The stress based criteria rely on the viewpoint that a semi-solid body will fracture if the applied or induced stress exceeds the critical strength of the body. Many stress based criteria have been proposed and modified [9]. For instance, Lahaie and Bouchard [13] extended the simple fracture stress model and developed a comprehensive hot tearing model, which involves solid fraction (f_s), strain and microstructural parameter. The fracture initiation stress ρ_i is proposed as:

$$\rho_i = \frac{4\gamma}{3h}\cdot\left(1+\left(\frac{f_s^m}{1-f_s^m}\right)\varepsilon\right)^{-1} \tag{1}$$

Where γ is the surface energy of liquid, h is the thickness of liquid film, m is a microstructural dependent parameter, ε is the accumulated strain. The larger $\rho_i$is, the less the ingot is prone to hot tearing.

The trend of calculated fracture stress as a function of solid fraction (f_s) corresponds well with the experimental data. However, the calculated fracture strain disagrees with the collected experimental data presented by Eskin et al. [9]. The calculated fracture strain decreases linearly with the f_s while the experimental determined fracture strain shows a U-shaped dependence of f_s. Thus, Lahaie's criterion has its limitation, as it neglects the effect of feeding on the liquid flow and healing of the tears. It is assumed that similar disagreement between the calculated strain with Lahaie and Bouchard's criterion and experimental strain will be found for Mg alloys.

2.1.2. Critical strain based criterion

It is suggested that the strain/strain rate is more critical for hot tearing than stress [14]. The studies on residual strain/stress show that the tensile stress is not required to generate hot tears, only tensile strain is sufficient to form a hot tear. The strain based criteria compare the proposed critical strain and the experimental measured ductility of the alloy. If calculated critical strain is higher than the experimentally determined fracture strain, hot tearing will occur.

Magnin et al. [15] proposed the greatest positive principle plastic strain εp^{ii}_{max} as the critical strain (hot tearing index). Their calculations show that the maximum εp^{ii}_{max} appears at the centre of the billet (DC casting of Aluminium alloys) and depends on the casting speed. Such prediction is in good agreement with the casting practice: the centre of the billet is more prone to hot tearing and a high casting speed leads to high HTS. The constraint of Magnin's approach is the validation of the model requires ductility profile of an alloy in the semi-solid range. Such ductility profile is rarely available for most alloys, especially for Mg alloys. Thus, the precise prediction of HTS for Mg alloys with Magnin's criterion relies on the ductility database of Mg alloys.

2.1.3. Critical strain rate based criteria

Rappaz, Drezet, and Gremaud [16] (RDG criterion) proposed a hot tearing criterion based on the maximum strain rate ($\dot{\varepsilon}_{\max}$) that the mushy zone can sustain before the hot tear occurs. The hot cracking sensitivity (HCS) is defined as $\dot{\varepsilon}^{-1}_{\max}$. The $\dot{\varepsilon}_{\max}$ is written as:

$$\dot{\varepsilon}_{max} = \frac{G^2\lambda_2^2}{180(1+\beta)B\mu\Delta T_0^2}\Delta p_{max} - \frac{v_T G\beta A}{(1+\beta)B\Delta T_0} \tag{2}$$

where G is the temperature gradient; λ_2 is the secondary dendrite arm spacing; β is the shrinkage factor; μ is the viscosity; ΔT_0 is the solidification interval; Δp_{max} is the maximum pressure drop the mushy zone can bear; $v_T$is the velocity. The two integrals A and B depend only on the nature of the alloy and its solidification path, i.e. on the relationship between f_s and T. They are also extremely sensitive to the choice of integral limits.

Among all the required parameters, $\Delta p_{max}$is a key value. The Δp_{max} (also called cavitation depression) is set as 2 kPa for Al-Cu alloys and the calculated HCS agrees with the casting practice. It is unknown that whether 2 kPa is a suitable value for Mg alloys. The cavitation depression is around 90 kPa for stainless steel [17]. The RDG criterion showed an acceptable ability to predict crack occurrence in arc welding of stainless steel. Similarly, the RDG criterion is also applicable to precisely predict the tearing occurrence in Mg alloys in the future. However, the cavitation depression for Mg alloys still needs to be determined.

The RDG criterion takes both solidification shrinkage and deformation induced fluid flow into account. According to Suyitno's evaluation [18], RDG criterion shows the greatest potential in the qualitatively prediction of HTS. However, the RDG criterion does not involve the propagation of hot tearing and it is derived from columnar dendritic grain structure.

Braccini et al. [19] attempt to extend the RDG model with incorporation of the propagation of hot tearing. Grandfield et al. [20] also proposed a model based on the RDG model which takes the equiaxed grain structure into consideration. Both Braccini and Grandfield's criteria are still not able to predict the hot tearing quantitatively. Further improvement for the hot tear prediction should involve an approach that lead to better predictions of whether hot cracks will be formed during actual casting. Besides, these two criteria are also not applicable to Mg alloys at present. Because Braccini's criterion also requires cavitation depression and Grandfield's criterion requires surface tension, which is not available for most Mg alloys.

2.2. Non-mechanical based criteria

2.2.1. Clyne and Davies's criterion

In 1975, Clyne and Davies [21–23] proposed a hot tearing theory, which considers the critical time spent during solidification when the structure is most vulnerable to cracking. They suggest that the interdendritic separation stage is most susceptible to hot tearing with a solid fraction between 0.9 and 0.99 and the stress can be released at a solid fraction between 0.4 and

0.9. The proposed crack susceptibility coefficient (CSC) is defined as:

$$CSC = \frac{t_V}{t_R} = \frac{t_{0.99} - t_{0.9}}{t_{0.9} - t_{0.4}} \quad (3)$$

where t_V is the vulnerable time period where hot tearing may develop and t_R is the time available for the stress-relief process where mass and interdendritic feeding occur. $t_{0.99}$, $t_{0.9}$, and $t_{0.4}$ correspond the time when the local solid fraction (f_s) is 0.99, 0.9, and 0.4, respectively.

Clyne and Davies's criterion has been applied to several magnesium alloy systems to predict their HTS [24–26]. The predicted results and the experimentally determined HTS (crack volume) of binary Mg-Zn alloys are compared and shown in Fig. 1 [27]. Both the prediction and the experimental results follow the so called "Λ" shape. The HTS increases with increasing in the content of alloy elements and then decreases with further increasing in the content of alloy elements. Similar results are also found in Mg-Al [28], Mg-Y [25] and Mg-Ca [26] alloys proving that the Clyne and Davies's criterion can successfully predict the compositional dependence of hot tearing.

However, Clyne and Davies's criterion still has several limitations. Firstly, the criterion uses a fixed equation to estimate the cooling rate and thus does not incorporate the influence of initial mould temperature. In the casting practice, the HTS of Mg-Zn alloys decreases considerably with increasing the mould temperature (Fig. 1). Secondly, their calculation does not consider the influences of microstructure and material properties on HTS. In fact, both microstructure and mechanical properties in the semi-solid state plays an important role on their hot tearing behaviour. With these limitations, the predicted CSC is not sensitive to the casting speed and the tearing location, which disagrees with the casting practice.

2.2.2. Suyitno's criterion

Suyitno et al. [29] proposed a hot tearing criterion combining critical liquid feeding theory, deformation rate, and cavity formation. In principal, the contribution of feeding, shrinkage and deformation to the cavity are calculated and compared. If the net results of contributions are positive, the cavity will form which may finally lead to the formation of a hot tear. Whether the cavity propagates to a tear depends on critical diameter of the cavity and thus on the stress developed in the mush.

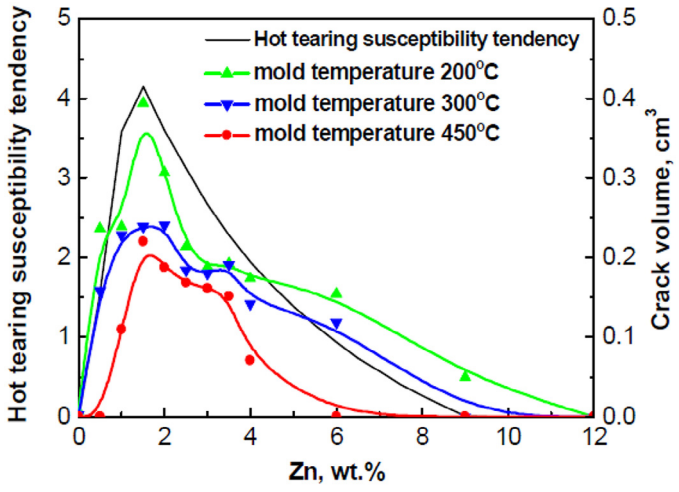

Fig. 1. Comparison of the calculated CSC value (hot tearing susceptibility tendency) and the experimental determined crack sizes of binary Mg-Zn alloys [27].

Among the existing hot tearing criteria, only the Suyitno's criterion adequately responds to all tested parameters, such as casting speed, ramping rate, grain size, and location of tear in a billet [12]. The model is unique as it can distinguish whether a hot tear or a micro-porosity appears under a certain strain rate. Most criteria are proposed to evaluate the HTS of an alloy. However, the precise prediction requires several parameters, such as Young's modulus of the mush, surface tension between liquid and solid, and permeability of the mush, which are rarely available, especially in Mg alloys. These parameters need to be determined experimentally. However, the existing experimental techniques are not reliable [5]. Consequently, the widespread utilization of Suyitno's criterion in Mg alloys is limited.

2.2.3. Kou's criterion

Recently, Kou [30] proposed a criterion for cracking during solidification. It assumes that the tear initiates when the net expansion of the intergranular space exceeds liquid feeding. The net expansion consists of the space moved under tension and the space expansion induced by grain growth. With the assumption that the hot tearing occurs near the end of solidification ($\sqrt{f_s} \to 1$), the condition of hot tearing is expressed as:

$$\left\{ \frac{d\varepsilon_{local}}{dT} > \sqrt{1-\beta}\frac{d\sqrt{f_s}}{dT} + \frac{1}{(dT/dt)}\frac{d}{dz}\left[\left(1-\sqrt{1-\beta}\sqrt{f_s}\right)v_z\right] \right\}_{\sqrt{f_s}\to 1} \quad (4)$$

where ε_{local} is the local strain, T is the temperature, β is the solidification shrinkage, f_s is the solid fraction, dT/dt is the cooling rate, z is the growth direction of the columnar dendritic grain, v_z is the velocity of intergranular liquid flow in the negative z-direction. The index of hot tearing is proposed as $|dT/d(f_s^{1/2})|$ near $(f_s)^{1/2} = 1$.

As validated in several binary Al alloy systems [31,32], Kou's criterion is successfully applied to predict the compositional dependence of hot tearing. Kou's criterion is fully applicable to predict the compositional dependence of HTS for Mg alloys, as the required parameters are easy to obtain. However, the accuracy of prediction with Kou's criterion highly depends on the selection of the solid fraction range. There is no theoretical basis on how to choose the solid fraction range for each alloy. The empirical selected range varies from one alloy to another, which restricts its application. Besides, Kou's criterion shows no sensitivity to casting speed and cannot predict whether a hot tear will form.

2.3. Comparison of hot tearing criteria

According to Suyitno et al.'s [18] and Eskin's [9,12] evaluation, only the Suyitno's criterion adequately responds to casting practice. Suyitno's criterion gives a precise prediction of whether a hot tear will form under a certain solid fraction and strain rate. However, it requires parameters that are rarelyavailable and difficult to determine with the existing

experimental techniques. Clyne and Davies's and Kou's criteria have easy access to the parameters needed for the calculation. All parameters are easily calculated from commonly used thermodynamic software, i.e. Pandat and well-developed database PanAl and PanMg. Hence, these two criteria can be used to predict the HTS of Mg alloys and can successfully provide the "Λ" curve. The limitations of these two criteria are that they show no sensitivity to casting speed and cannot predict whether a hot tear will form. Thus, the selection of a proper criterion depends on the availability of required parameter and the expectations of the predictions. For instance, if the compositional dependence of hot tearing is of most interest and all the parameters required are available, Clyne and Davies's criterion is a good choice. However, a new hot tearing criterion is still in need.

3. Numeric simulation of hot tearing

The application of numerical simulation techniques in metal casting has provided insights into understanding the effects of alloy chemistry, thermal-fluid transport phenomena, and their relationship to the alloy microstructure and the formation of defects [33]. It reduces the time required for new product design cycle and can be used as a tool for quality assurance. The complexity of mushy zone makes the hot tear modelling even more demanding [34].

Several hot tearing criteria have been implemented in a finite element simulation of metal casting with the commercial software, such as ProCAST [35–37], MAGMAsoft [38], and ABAQUS [39], etc. Both ProCAST and MAGMAsoft have been applied to predict the HTS of Mg alloys. It is reported that the hot tearing model implemented in ABAQUS has been applied and validated in steel. A recently developed three dimensional (3-D) granular model to simulate the formation of hot tearing is also reviewed in this section.

3.1. ProCAST

The commercial numerical simulation software ProCAST simulates the process of casting and solidification based on finite elemental method. ProCAST has been extensively used in foundries to understand the physical phenomena occurred during solidification. In this software, two modules can be used to predict hot cracking [40]. One is called HCS, which is based on the RDG criterion. The detailed description of RDG criterion can be found in section 2.1.3. The other is hot tearing indicator (HTI), which is based on Gurson's constitutive model. According to the manual of ProCAST [40], HCS is only suitable for steady state conditions, as encountered in continuous (or DC) casting. HTI should be used to compare different designs with the same alloy.

The HTI is a strain-driven model based upon the total strain which develops during solidification. The model computes the elastic and plastic strains at a given node when the fraction of solid is between the critical solid fraction (usually 50%) and 99%. The HTI (e_{ht}) was obtained as follows:

$$e_{HT} = \bar{\varepsilon}_{ht}^{p} = \int_{t_c}^{t} \dot{\varepsilon}^{P} dt, \quad t_C \le t \le t_S \tag{5}$$

where $\bar{\varepsilon}_{ht}^{p}$ is the critical accumulated effective plastic strain for the initiation of hot tearing, $\dot{\varepsilon}^{p}$ is the effective plastic strain rate, t_C is the time at the coherency temperature, and t_S denotes the time at the solidus temperature.

Wang et al. [36,37] simulated the HTI of Mg-Y and Mg-Zn-Y alloys with ProCAST. The simulation and experimental results of Mg-Zn-Y alloys were compared in Fig. 2. Simulated location of hot tears and the severity of hot tearing are in agreement with the casting practice. Besides, the simulation results of both Mg-Y and Mg-Zn-Y alloys indicate that the HTI decreases with increasing mould temperature. Such simulation results are in line with the hot tearing tests. Good agreement between the simulation and experimental results is also obtained in Mg-Al alloys [35].

However, the accuracy of the simulation highly depends on the existing database of Mg alloys. It is found in Mg-Ca alloys, although the location and the severity of hot tearing are in agreement with the experimental results, the simulated HTI at two mould temperatures (250 °C and 450 °C) have minor difference. In fact, the hot tearing tests show that the HTS decreases dramatically with increasing the mould temperature. Such disagreement is due to the lack of stress hardening data of Mg-Ca alloys at semi-solid state in the existing database, such as yield strength. Without the yield strength profile, the simulation has zero contribution from plastic strain which most likely results in the disagreement. Thus, in order to improve the accuracy of simulation, it is obliged to complete the mechanical property database of Mg alloys in the future.

The HTI module in ProCAST is capable of simulate the HTS of Mg alloys. The simulated HTI is composition dependent and sensitive to the initial mould temperature if the stress hardening data is available. As a result, the application of HTI module is restricted to the well-investigated alloy systems which have the complete database of mechanical property. Besides, the value of simulated HTI is not comparable in different alloy systems.

3.2. MAGMAsoft

A viscoplastic deformation model was used to predict hot tears in an AZ91D permanent mould casting with MAGMAsoft [38]. The viscoplastic model calculates material damage as well as solid deformation. The porous damage is defined the same as hot tearing indicator used in ProCAST.

The predicted damage from the simulations was found to be in good agreement with the hot tears observed in the experiments, both in terms of location and severity, as shown in Fig. 3. The simulation also reveals that the porous damage is mould temperature dependent, which is in line with casting practice.

The viscoplastic model in MAGMAsoft is able to simulate the HTS of Mg alloys, but it has the same limitations with the HTI module in ProCAST.

3.3. A new three dimensional granular model

Recently, a 3-D granular hydromechanical coupled model has been developed to predict hot tear formation in solidifying alloys with globular microstructures [41,42]. This model predicts the overall response of semi-solid alloys to an externally

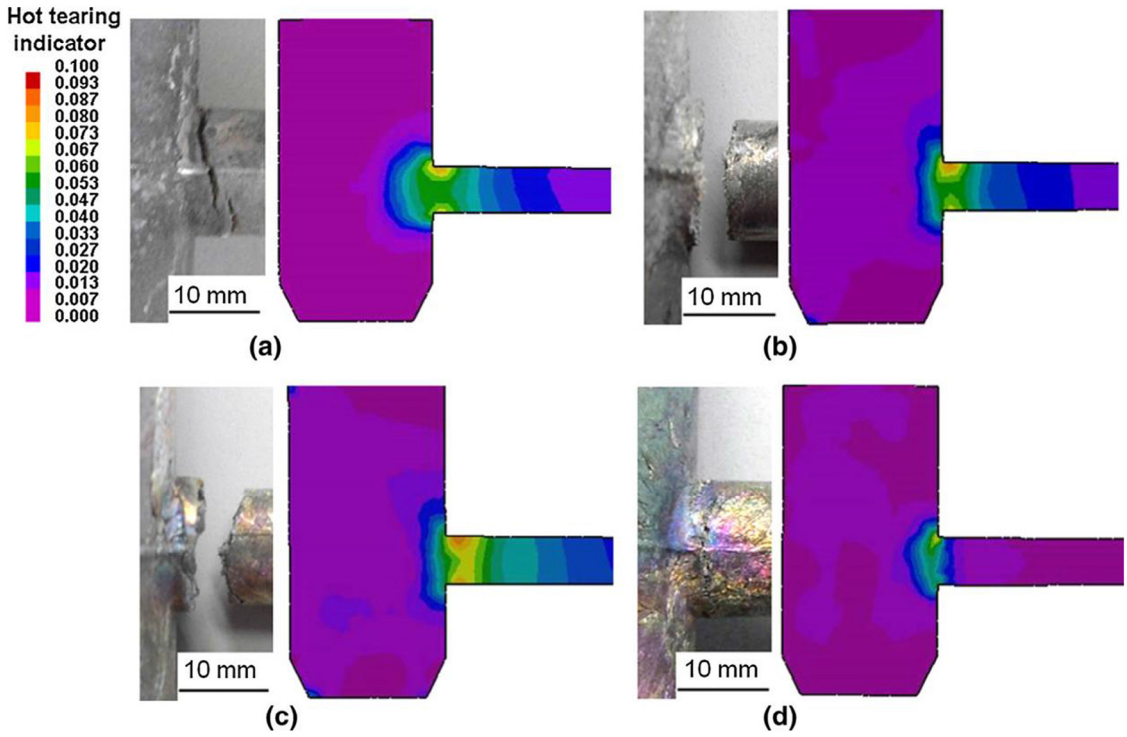

Fig. 2. Comparison between the simulation results of HTI and experimental observations for Mg-4.5Zn-xY alloys at the mould temperature of 250 °C, (a) x = 0, (b) x = 0.4, (c) x = 0.9, and (d) x = 2 [36].

applied strain before and after initiation of fracture. It is an advanced model since it considers the localization of strains and feeding at grain boundaries. Such localization has been clearly demonstrated by *in situ* X-ray tomography tensile testing. The hot tearing criterion used in this model is an extension of RDG criterion. In principal, it is considered that the hot crack starts to initiate in a liquid channel connected to the atmosphere once the liquid pressure p_l reaches a critical pressure p_l^c. The liquid pressure p_l in the semi-solid medium is computed through a finite element code to solve the following equation:

$$\frac{2h^3}{3\mu_l}\nabla^2 p_l = 2\beta v^* + \Delta v_{sn} + \frac{2h}{k_l}\frac{\partial p_l}{\partial t} \tag{6}$$

Where h is the half-width of the liquid channel, μ_l is the dynamic viscosity of the liquid, β is shrinkage factor, v* is the solidification speed of the solid liquid interface, v_{sn} is the normal velocity difference of the solid grains, and k_l is the bulk modulus of the liquid.

And the critical pressure p_l^c is given by:

$$p_l^c = p_a - \frac{\lambda \cos\Theta}{h} \tag{7}$$

Where p_a is the pressure of atmosphere, λ is the surface tension at the void–liquid interface, Θ is the dihedral angle, h is the same as defined previously.

The results of a granular model have been validated with *in situ* X-ray tomographic observations made during the tensile deformation of a mushy Al-Cu alloy specimen, as shown in Fig. 4. Good agreement is obtained between modelling and experiments. The modelling reveals that the specimen continuously necks, allowing the liquid channels perpendicular to the tensile axis to open by feeding them with the liquid coming from neighbouring zones and from channels which are parallel to the tensile axis and tend to close. Once the liquid is no longer able to feed the deformed zone, cracks form in the structure. The granular model also demonstrates that the grain size has a large effect on the "overpressure" required to overcome the capillary forces at the liquid–void interface. It shows that the HTS increases with increasing grain size.

The 3-D granular model is an advanced hot tearing model and shows a great potential to accurately predict the formation of hot tearing. However, the model is applicable to well-investigated alloys, such as Al-Cu alloy. The application of the 3-D granular model to Mg alloys is still limited at present, as the parameters required for the simulation with this model are seldom available. Besides, the validation technique, *in situ* X-ray tomography technique, also needs to be developed for Mg alloys.

4. Experimental methods to evaluate hot tearing susceptibility

Many set-ups have been developed to investigate hot tearing behaviour of alloys in the past decades. Different apparatuses use different constraints to induce stress which promote the formation of hot tearing. The typical apparatuses including the recently developed *in situ* set-ups are summarized in this section. Some of the apparatuses have been applied to hot

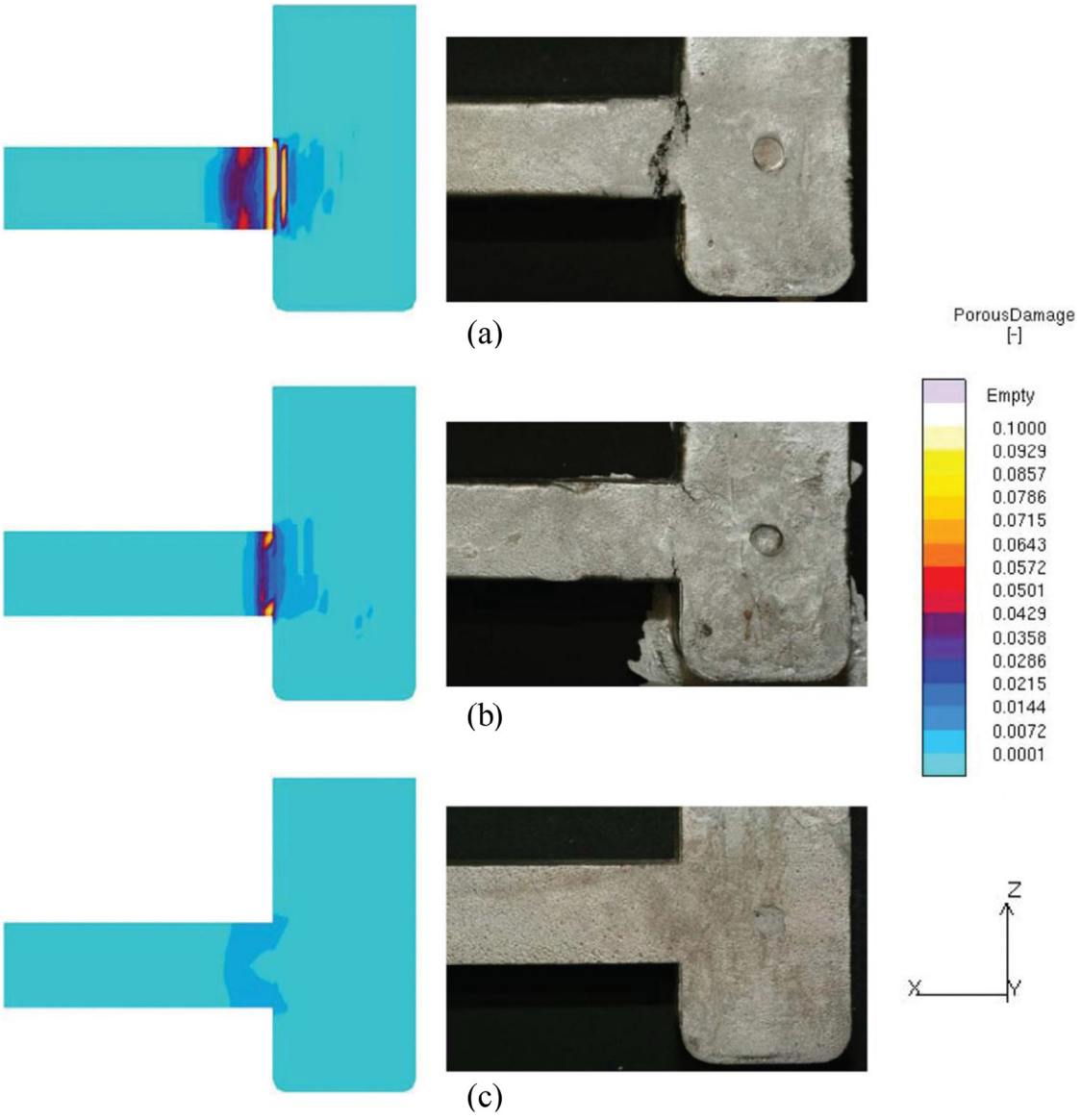

Fig. 3. Comparison of simulation results and the corresponding experimental results with the initial mould temperature of (a) 140 °C, (b) 260 °C, and (c) 380 °C [38].

tearing studies of magnesium alloys. The evaluation methods of hot tearing susceptibility are summarized as well.

4.1. Ring mould testing

Ring mould has been used by many researchers to assess the HTS of Mg alloys [43–47]. Wang et al. [47] used a crack-ring mould to study the hot tearing behaviour of Mg-9Al-(0–1)Zn alloys. The set-up consists of a round mould with a diameter of 108 mm, two round steel, and two steel chills, as shown in Fig. 5 [47]. Round steels with a series of diameters (93 mm, 98 mm, 103 mm, etc.) are used to constrain the solidification shrinkage of alloys. The stresses derived from constrained shrinkage promote the formation of hot tears. The severity of hot tearing (hot tearing susceptibility coefficient, HSC) is expressed as:

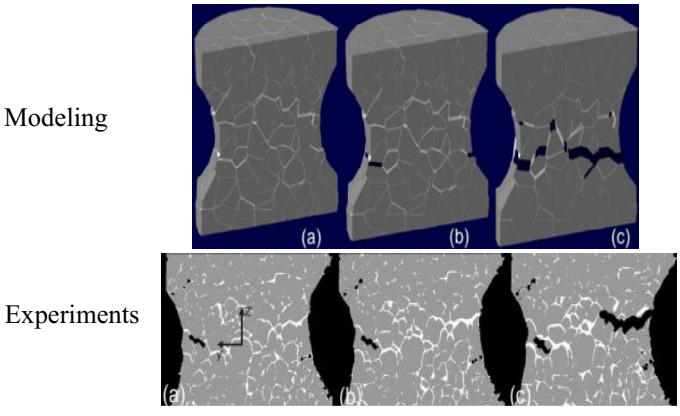

Fig. 4. Comparison between granular modelling and experiments, (a) t = 405 s for modelling, t = 486 s for experiments, (b) t = 729 s, and (c) t = 1215 s [41].

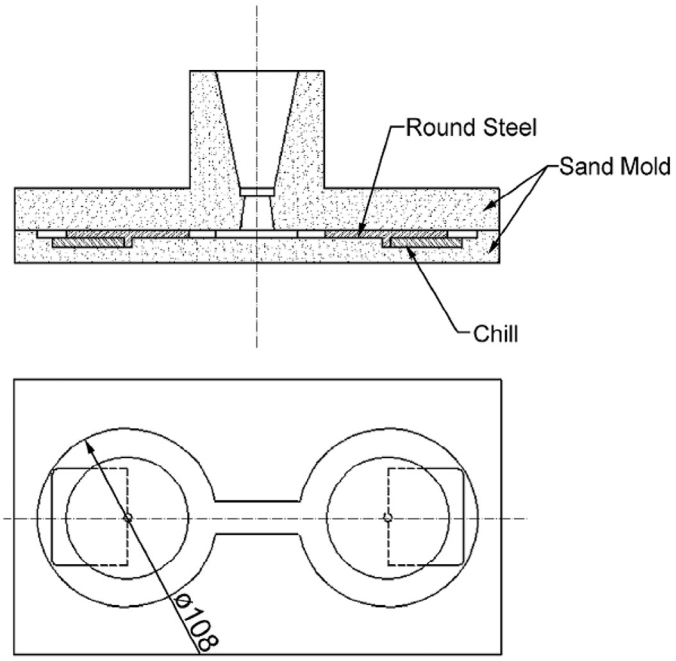

Fig. 5. Mould of crack-rings [47].

$$HSC = \frac{108 - D_{crit}}{108} \quad (8)$$

where D_{crit} is the critical diameter of the round steel, which is defined as the diameter at which the sample begins to crack.

Ring mould is a simple and classic set-up which can be used to briefly compare the HTS of alloys. The constraint of this set-up is that it gives limited information about the formation of hot tearing, as it only provides the tear under a certain cast condition.

4.2. Constrained rod casting testing

In principle, the constrained rod casting (CRC) set-up consists of rods with constrained shrinkage and thus induce tension. Such induced stress may results in the formation of hot tearing [48]. There are two types of constrained rod casting moulds using the rods either have different lengths or diameters.

4.2.1. Bars with different length

Permanent star-shaped mould (PSM) uses rods with different lengths. P. Gunde et al. [49] investigated the hot tearing behaviour of Mg-Zn-Y alloys with a PSM. The schematic PSM mould [9] and a typical casting [49] are shown in Fig. 6. Severity of hot tearing is expressed as HTS_{PSM}. A number with a value between 0 and 1 was assigned by examining each rod according to the following scheme: 1 for completely broken rods; 0.5 for obviously cracked rods; 0.25 for rods with cracks detectable only with the magnifying glass; and 0 if no cracks were observed. The final HTS_{PSM} is the average value of all the rods.

PSM produces reliable hot tears as it contains several bars which reduce the impact of random conditions on the HTS of an alloy. However, the evaluation of HTS only gives a brief estimation of severity of hot tearing.

To overcome the limitation of HTS evaluation method of PSM, Cao et al. [28] improved the method in another commonly used CRC mould (Fig. 7 [28]). The CRC mould consists of parallel rod with different lengths. The crack width length instead of ranking the crack with a number is used in the new evaluation method. Besides, the location factor and the length factor are taken into consideration. The hot cracking susceptibility (HCS) is defined as:

$$HCS = \sum w_{crack} f_{length} f_{location} \quad (9)$$

In the above equation, crack width factor w_{crack} is the maximum crack width. The length factor and location factor is assigned with a number according to the tearing difficulties [28], respectively.

4.2.2. Bars with different diameter

Fig. 8 shows the second type of the CRC mould which contains rods with different diameters. This mould was used to investigate the hot tearing behaviour of Mg-Al-Mn-Sr alloys [50]. The hot crack occurs most likely in the area between the upper and middle column, as such area bears the maximum contraction stress during solidification. Rods with small

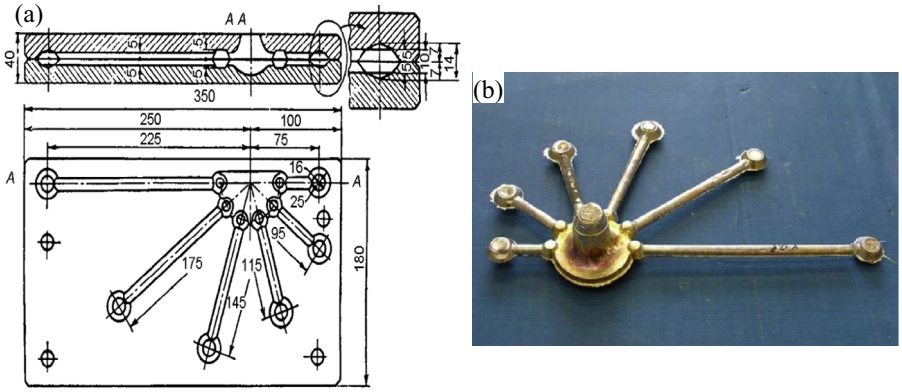

Fig. 6. (a) Schematic mould of PSM [9] and (b) a typical casting [49].

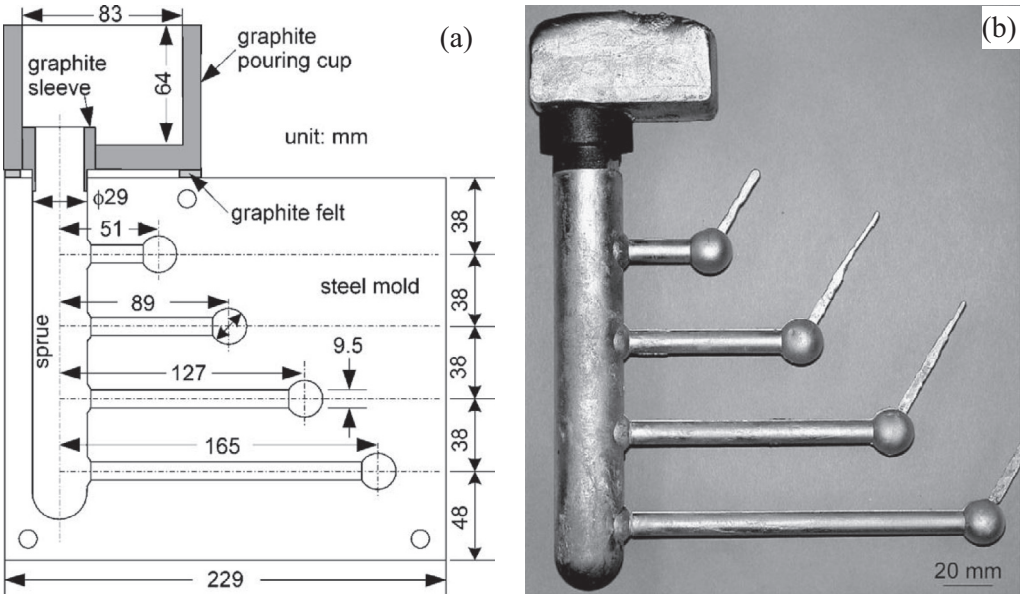

Fig. 7. Another constrained mould casting, (a) schematic mould, (b) casting [28].

diameter are more prone to hot tearing than rods with large diameter. Thus, the hot crack grade (represents the hot tearing susceptibility (HTS)) for this mould is proposed as:

$$HTS = \Phi^2 \tag{10}$$

where Φ is the maximal diameter of middle column where hot cracks occurred. Higher value of the hot crack grade indicates a high HTS of the alloy.

It is easy to carry out hot tearing tests with all kinds of CRC moulds. The obtained HTS is reliable and comparable. However, the limitation of these set-ups is they only produce hot tears with different severity. They are unable to provide more information about hot tearing, such as when the tear forms, at what temperature the tear forms, etc.

4.3. Instrumented constrained rod casting testing

To overcome the limitation of the simple CRC mould, more sophisticated apparatuses have been developed. In general, the temperature, load, time, and displacement are simultaneously recorded during solidification process. These recorded data help to clarify the initiation and propagation of hot tearing.

4.3.1. Apparatus records the load

Cao et al. [51,52] added a bar with temperature and load acquisition units to the original CRC mould (Fig. 7), as shown in Fig. 9. By analysing the recorded load–time–temperature curve, the characteristics of hot tearing including the initiation, the evolution and final size of the hot crack and so on can then be clarified.

Zhen et al. [53] simplified and extended Cao et al.'s modified CRC mould. Only one rod is used in Zhen et al.'s mould, as shown in Fig. 10. Besides, the rod portion of the mould was designed with a taper. This unique design successfully eliminated the influence of friction between the mould and casting rod on hot tearing behaviour. As a result, the collected contraction force data are more reliable. A typical recorded force–time–temperature curve of Mg-0.5Ca alloy cast at a mould temperature of 250 °C is shown in Fig. 11 [26]. The force drop

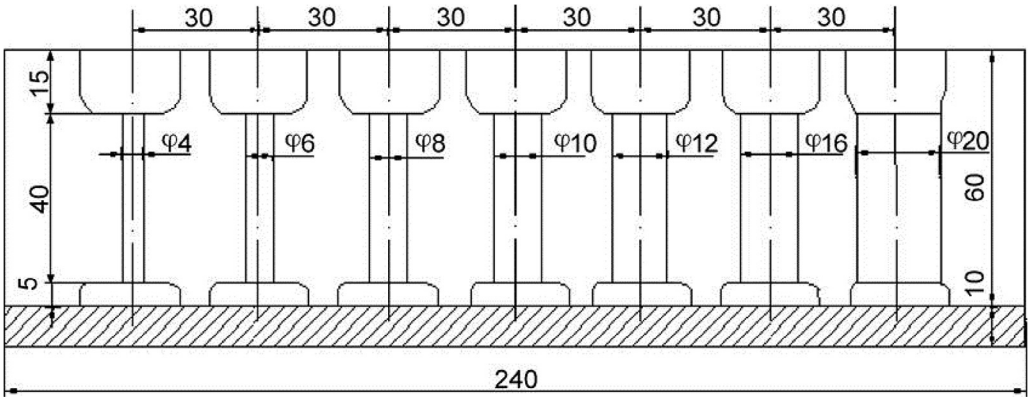

Fig. 8. Schematic CRC mould with different diameter [50].

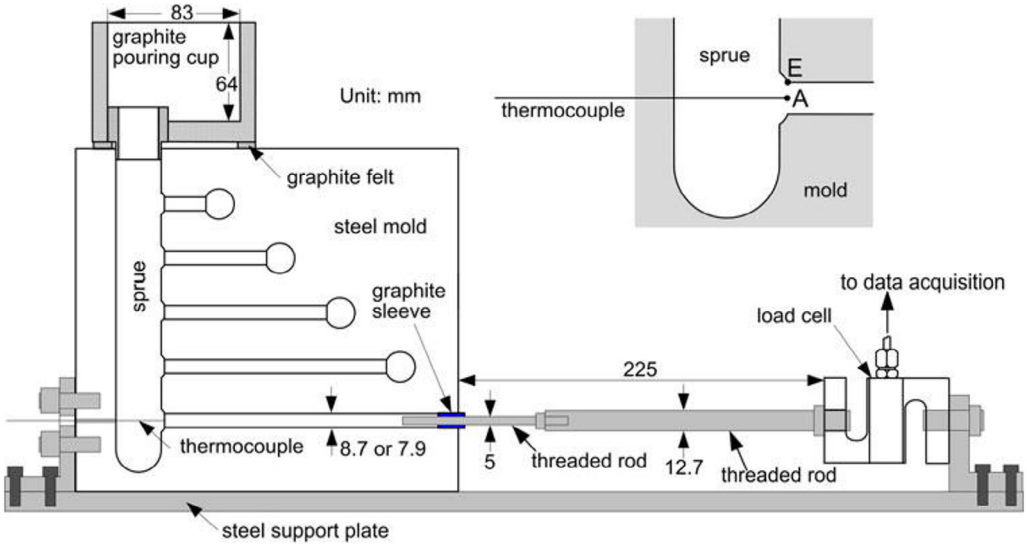

Fig. 9. Instrumented CRC mould from Cao and Kou [52].

is considered as the initiation of hot tearing. Through the force drop, the temperature and the solid fraction of the tearing initiation are determined. Such solid fraction is essential for clarifying the hot tearing mechanism.

Zhen et al.'s apparatus has been applied to hot tearing studies of several magnesium alloys, such as Mg-Al [54], Mg-Zn [24], Mg-Gd [55], Mg-Y [25], Mg-Ca [26], etc. Crack volume is used as the index of HTS in their studies. The crack volume is more accurate than the crack size used in the previous research, since it takes the depth of crack as well as the complexity of the crack pattern into account [54]. Normally, the volume of cracks is measured by a wax penetration method. However, this wax method can only measure the volume of open cracks. More recently, X-ray tomography technique is introduced to measure the crack volume. The volume of both open and closed cracks is included [25,55].

4.3.2. *Apparatus records the displacement/load*

Another approach to improve the simple CRC mould is to measure the load/displacement of the rod during solidification. Metal Processing Institute at WPI and CANMET Materials Technology Laboratory developed an instrumented constrained rod mould [56,57], as shown in Fig. 12. The recorded load is similar to the load measured in Cao et al.'s and Zhen et al.'s apparatus, which helps to determine the initiation of hot tearing. The displacement was measured in the unrestrained rod which represents the linear contraction when the rod was relaxed. Such displacement is found to correlate to HTS of the alloy. Extremely low displacement before the non-equilibrium eutectic temperature was detected in tear-free alloy. Much high displacement was measured in the alloy with major hot tear. The hot tearing index is defined as the crack area, which is determined with image processing software (Image J).

Valuable information about the formation of hot tearing is provided by the instrumented CRC mould set-ups. The simultaneously measured temperature, time, load, and displacement helps to understand the mechanism of hot tearing. Further improvement of these set-ups can focus on the *in situ* observation of the formation of hot tearing.

4.4. In situ *observation of hot tearing*

Recently, *in situ* observation of hot tearing formation has drawn extensive attention of related researchers [58,59]. Video camera as well as synchrotron X-ray has been introduced to observe the *in situ* formation of hot tearing.

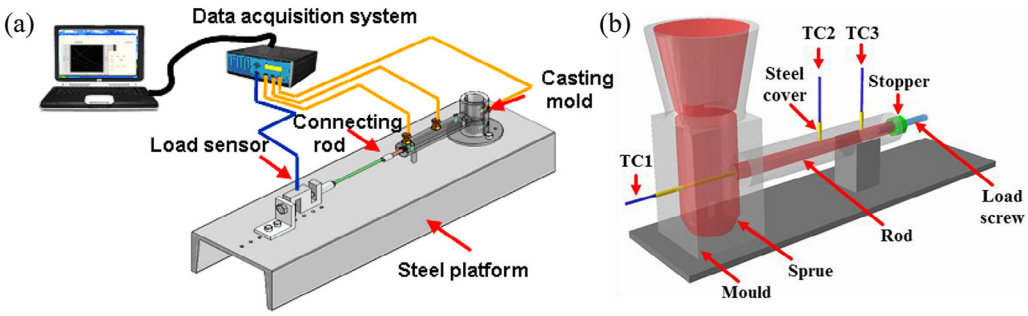

Fig. 10. Schematic diagram of the apparatus, (a) the complete apparatus, (b) close-up of CRC mould (TC-Thermocouple) [26].

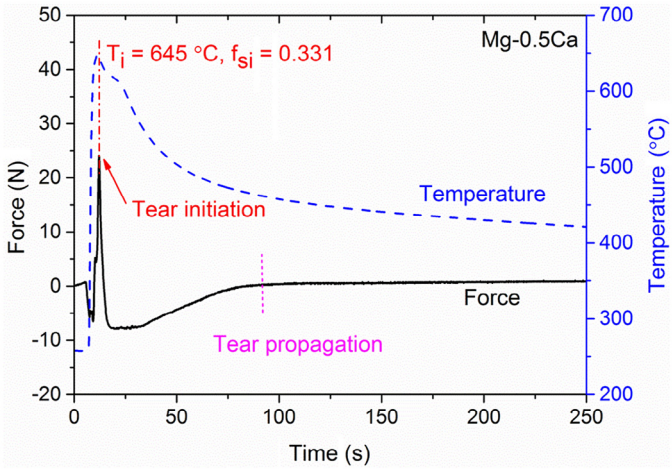

Fig. 11. A typical force–time–temperature curve of Mg-0.5Ca alloy [26].

4.4.1. Video camera

Video camera attached to the microscope was used to observe hot tearing formation of succinonitrile-acetone [58,60]. Tearing mechanisms were clarified. However, due to the difference between organic and metal alloys, the developed hot tearing mechanisms are not fully applicable to metal alloys.

Davidson et al. [59] added a video camera to the original hot tearing set-up, which enables *in situ* observation of the formation of hot tearing in Al-Cu alloys. As illustrated in Fig. 13, a mirror angled at 45° is positioned above the glass window. A video camera with a long focal length lens is used to record the images to digital tape at the standard 25 frames s^{-1} interlaced. Through the direct observation of the hot tearing initiation and propagation, it is concluded that the hot tearing formed with a solid fraction between 93% and 96%. In addition, it is also observed in many cases that the tearing occurs away from the cold edge.

4.4.2. Synchrotron X-ray

Another possible approach to observe *in situ* formation of hot tearing is using the X-ray microtomography. It is attempted to perform semi solid deformation under tension with the highly focused and intense X-ray beams imposed on the hot spot area. Three dimensional (3D) tomographic volumes of the hot spot area are then reconstructed and provide detailed information on the initiation and propagation of the tear. Besides, 3D liquid/solid configurations and the interactions of tears with the microstructure can be observed as well.

In situ observation on deformation of semi-solid Al-Cu alloys under tension was carried out with the apparatus shown in Fig. 14 [41,61,62]. The specimen was heated to a temperature slightly above the eutectic temperature to reach semi solid state with a high solid fraction (above 0.9). Then, the tensile test was carried out at a deformation rate of 0.1 $\mu m \cdot s^{-1}$. During deformation, the specimen was continuously rotated through 180° in 16 s to acquire a series of 2-D radiographic projections at different angles. The projections were then processed to reconstruct a series of 3-D tomographic volumes with a pixel size of 2.8 μm.

It is found that during deformation the remaining liquid initially accumulates in a region such as at an intergranular surface nearly perpendicular to the tensile axis. The pores form in such region when the remaining liquid is drained. These pores are in fact interconnected and propagate as a void across the liquid surface. These observations clearly demonstrate that high-resolution X-ray tomography is valuable for the *in situ* study of hot tear formation in semi-solid alloys. Similar conclusions are obtained in *in situ* deformation study of commercial AA5182 (Al-4.63Mg-0.49Mn-0.17Fe-0.04Cu) alloy [63].

Puncreobutr et al. [64] used fast *in situ* synchrotron X-ray tomographic microscopy to study the influence of Fe-rich intermetallics on tearing formation of commercial A319 alloy (Al-7.5Si-3.5Cu, wt.%). Results show that the large fraction of β-intermetallics strongly blocks the interdendritic channels and induces porosity formation, and hence, increase the HTS. The porosity formation is owing to permeability reduction and hydrogen super saturation in the local subdivided domain.

In situ observation of hot tearing with video camera is a simple method with limitation. This technique can only observe the phenomenon occurred at the upper surface. On the contrary, *in situ* observation of hot tearing with synchrotron X-ray can overcome the limitation. Synchrotron X-ray microtomography

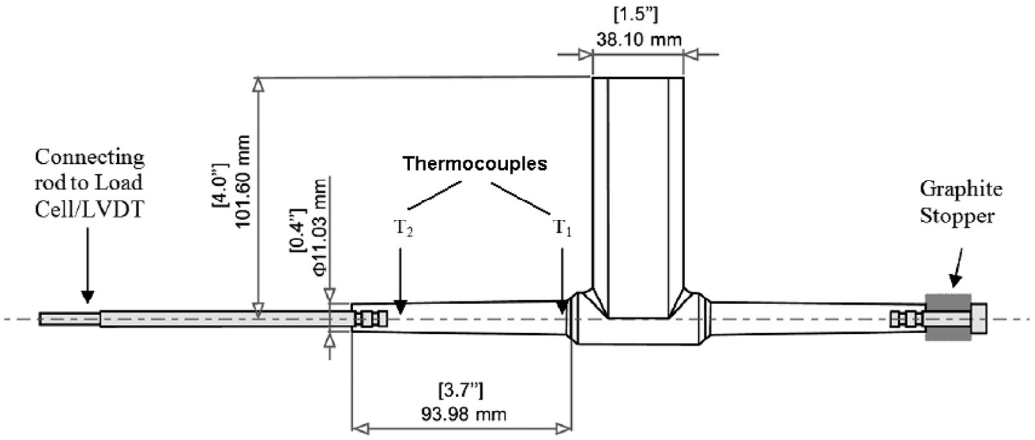

Fig. 12. Instrumented CRC mould from WPI and CANMET Materials Technology Laboratory [56].

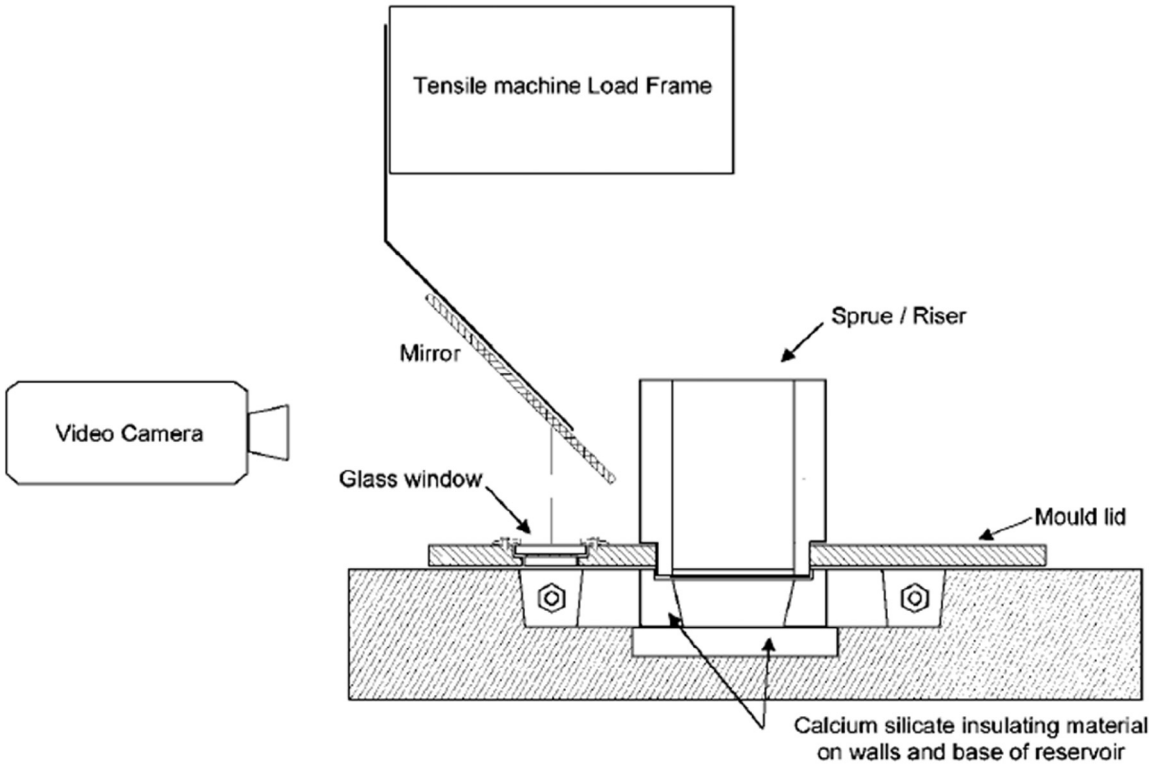

Fig. 13. Schematic of *in situ* observation of hot tearing by video camera [59].

provides 3D tomographic volumes and the inside is visible. However, the *in situ* observation of semi-solid deformation by synchrotron is mainly restricted in Al alloy. Utilization of such *in situ* observation on semi-solid deformation of magnesium alloys has not yet been reported in literature. One of the technical challenges in tensile test of magnesium alloys at semi-solid temperatures is the risk of fire since Mg alloys are prone to burning [65]. *In situ* observation of deformation of Mg alloys with X-ray tomography technique is an interesting topic in the future.

5. Factors influencing hot tearing

The hot tearing behaviour in metal castings has been experimentally investigated for many years with regard to the factors

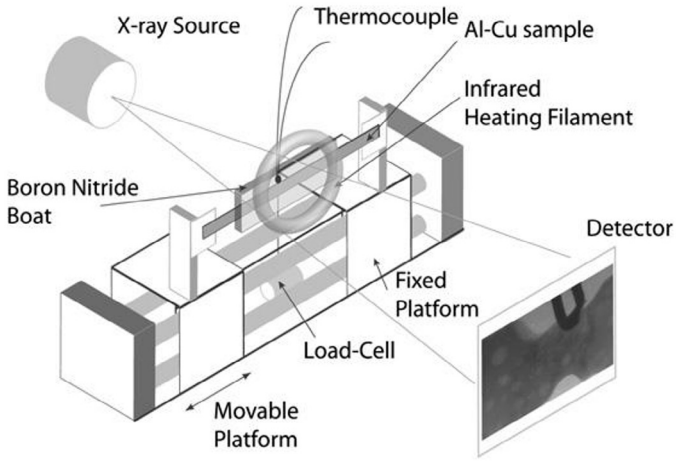

Fig. 14. Schematic of the semi-solid deformation apparatus [61].

that influence the HTS [21,51]. The factors are either alloy constitution or processing parameters related. Freezing range, amount of eutectic, the processing parameters include pouring temperature and initial mould temperature, grain size, and grain morphology play an important role on the hot tearing behaviour.

5.1. Alloy constitution

It is well established that super high purity metal is not prone to hot tearing [22]. Theoretically, a pure metal solidifies at a constant temperature and no tear would form. With a small amount of impurity (total Fe + Si = 0.03%), the high purity Al alloy exhibit a significant tearing [23]. It is concluded that the onset of hot cracking is at a very low solute content. The alloy with a small amount of solute solidifies within a temperature interval. At later stage in such solidification range (also called freezing range, FR), if the remaining liquid is difficult to flow through the interdendritic network, the pore or hot tears may occur under the accumulated stress/strain [20]. As a result, the binary or multi-component alloys which solidify in a temperature range might lead to the formation of hot tearing.

5.1.1. Binary alloys

As the majority of the binary Mg alloys displays eutectic, the following discussion focuses on the eutectic alloy system. The HTS of most binary alloys generally follows the "Λ" shape, as demonstrated in many Mg and Al alloys [11,24–26,28,47,51,55,66–69]. Fig. 15 (a) shows that hot tearing severity of various alloys increases with increasing in solute content and then decreases with further addition of solute. Alloying elements

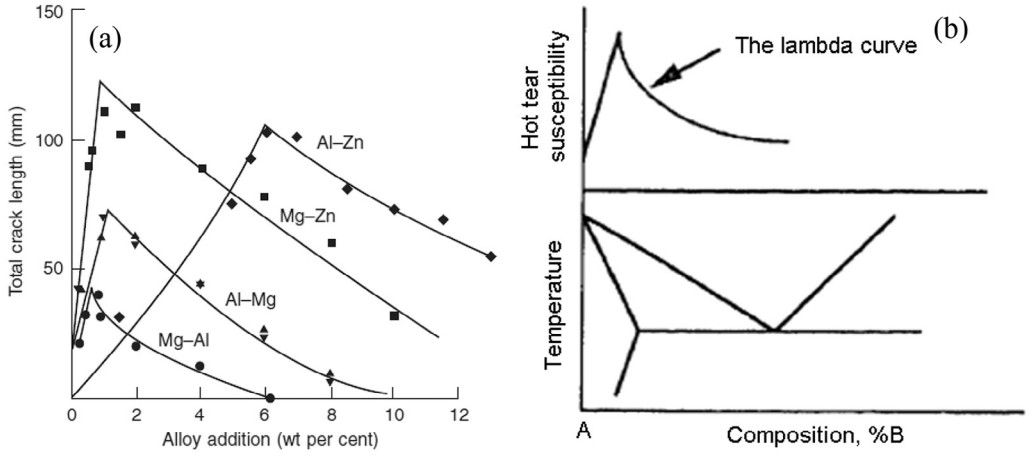

Fig. 15. (a) Hot tearing susceptibility of various alloys follow the "Λ" shape, crack length is determined from ring mould test [69], (b) Schematic illustration of the "Λ" shape of HTS and the correlation of HTS and phase diagram [69].

affected hot tearing in different ways. For instance, Mg-Zn alloys are more susceptible to hot tearing than Mg-Al alloys due to their wider freezing range. The shape and peak of the "Λ" curve is highly related to the phase diagram, as shown in Fig. 15 (b). Both freezing range and the amount of eutectic liquid are phase diagram dependent and play an important role on the HTS of the alloy.

The alloy with a larger freezing range is generally more prone to hot tearing. The reason for such correlation is that the alloy spends a longer time in the susceptible stage. The non-equilibrium freezing range (NEFR) and susceptible freezing range (SFR) of binary Mg-Ca alloys are presented in Fig. 16. The SFR ($T_{0.9}$-$T_{0.99}$) is defined as the temperature range in which the alloy is most susceptible to hot tearing with a f_s between 0.9 and 0.99. The phase diagram calculated from Pandat Software of Mg-(0–3) Ca alloys is also compared in Fig. 16. Both NEFR and SFR follow the "Λ" shape and the peak appears at Mg-0.1Ca and Mg-0.2Ca, respectively. As validated by the experimental hot tearing tests of Mg-Ca alloys, the peak susceptibility to hot tearing appears at Mg-0.5Ca [26]. As a result, SFR is a more reasonable factor to the practical HTS of Mg alloys than the NEFR.

The practical peak of HTS is also influenced by the amount of eutectic liquid. The presence of eutectic liquid is beneficial for hot tearing resistance when the amount reaches a critical value. A small amount of eutectic liquid aggravates hot tearing tendency [70]. The remaining liquid at the later stage of solidification distributes as thin liquid film at the grain boundaries. Tensile stress caused by contraction is highly concentrated in these liquid film areas to the extent that it may be sufficient to cause hot tearing. In the case of the alloy with a large eutectic liquid fraction, the liquid film is thick. Hence, the strain is essentially uniform and it is insufficient to cause a tear. Besides, the large amount of eutectic liquid can flow back to the tear region and thus heal the previously formed tear. Eutectic healing is clearly observed in various alloy systems with a high concentration of solute [25,26,55,71,72]. After the occurrence of hot tearing, the regions near them have a negative pressure. This negative pressure can suck back the liquid, and refill the tear [25]. The eutectic liquid fraction (f_{le}) in Mg-Ca alloys lineally increases with increasing the Ca content, as presented in Fig. 16 (b). The eutectic healing is mainly found in alloys with high content of Ca, such as Mg-1Ca and Mg-2Ca alloys [26].

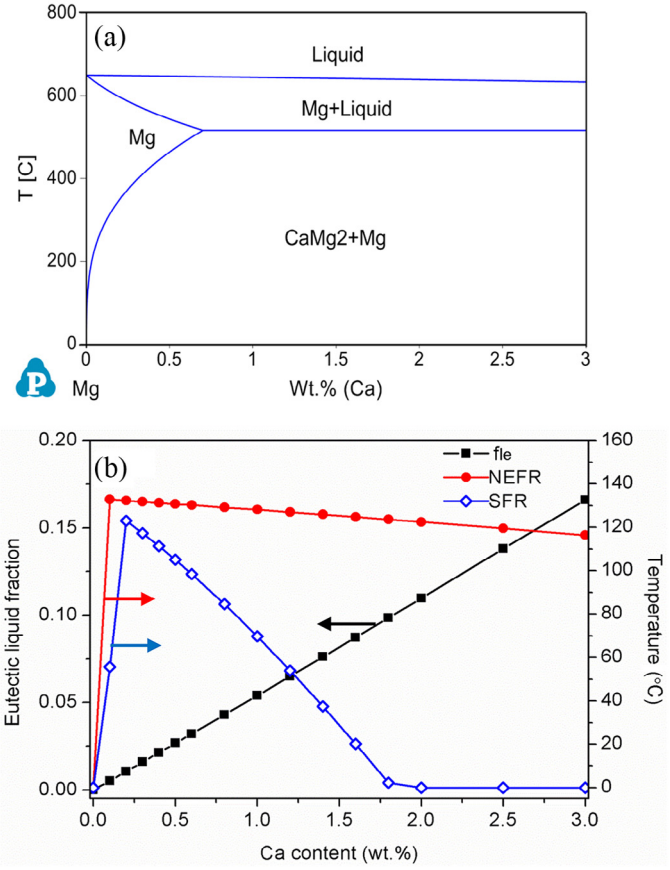

Fig. 16. (a) Phase diagram of Mg- (0–3) Ca alloys calculated from Pandat, (b) Non-equilibrium freezing range, susceptible freezing range and eutectic liquid fraction of Mg- (0–3) Ca alloys.

5.1.2. Multi-component alloys

The type and content of the alloying elements have complicated impact on the hot tearing behaviour of complex alloy systems due to their complicated solidification path. The hot tearing tendency of complex alloy systems does not follow the simple "Λ" shape. Researchers attempt to investigate the influence of Si:Mg ratio on the hot tearing behaviour of ternary Al-Si-Mg alloys [73]. The results indicate that the Si:Mg ratio is not critical to hot tearing. The dominant factors to hot tearing are FR and amount of eutectic. The low hot tear susceptibility of Al-Si-Mg alloys is either due to the shorter FR or the larger amount of final ternary eutectic. Similar results are also found in ternary Mg-Zn-Y [74] and Mg-Al-Ca [51] alloys that the high HTS is strongly related to the high FR and small amount of eutectic. It is expected that the HTS of multi-component alloy strongly depends on its FR and amount of eutectic.

5.2. Cast conditions

5.2.1. Pouring temperature

Contradictory results are reported on the effect of pouring temperature on the HTS of the metal alloys. Clyne and Davies's study show that high superheat (high pouring temperature) results in a high HTS [23]. Eskin et al. reported that an increase in pouring temperature decreases the vulnerability of the alloy to hot tearing [75]. Bichler et al. [76] presented that different pouring temperature does not have a significant effect on HTS in AZ91D alloy. Recently, Huang et al. [77] studied the effect of pouring temperature and mould temperature on HTS of AZ91D and Mg-3Nd-0.2Zn-Zr (NZ30). The results are presented in Fig. 17. It is found that the pouring temperature can affect the HTS only when the mould temperature is low. In addition, HTS decreases with increase in pouring temperature first, and then increases with further increasing pouring temperature. The effect of pouring temperature on HTS is not as significant as that of mould temperature.

Pouring temperature affects the HTS in two contrary ways [56]. On the one hand, high pouring temperature might spread the hot spot, which leads to reduced HTS. On the other hand, high superheat might increase the presence time of liquid film, which results in increased HTS.

5.2.2. Mould temperature

Investigations on several binary and ternary Mg alloys reveal that high mould temperature improves the hot tearing resistance [36,37,54,55,78,79]. The results of Mg-2Ca-xZn alloys clearly show that the HTS decreases dramatically with the mould temperature increase from 250 °C to 450 °C (Fig. 18).

Generally, high mould temperature improves the hot tearing resistance due to a reduction in thermal gradient and better compensation of strain [77]. During solidification, thermal gradients within the melt may result in regions of localized strain. Hot tearing occurs only if such accumulated thermal strain exceeds a critical value of strain in the casting [9,70]. Normally, a high initial mould temperature leads to a small thermal gradient and thus low localized strain. Solidification of a casting at a high initial mould temperature takes longer time, which provides adequate time to compensate for the accumulated strain [37]. However, the time for compensation may not be sufficient for a faster solidification process (low initial mould temperature). In addition, the solute segregation due to the fast cooling is likely to result in high HTS, as strain may concentrate on the solute segregated region.

5.2.3. Inclusions

The presence of MgO inclusions strongly destroys the continuity of the magnesium matrix and thus deteriorate the mechanical properties of alloys [80]. Oxide inclusions impede interdendritic feeding and reduce the wettability of the interdendritic fluid thereby having an adverse effect on hot tearing tendency [4]. Huang et al. [81,82] investigated the influence of inclusions on the HTS of Mg-10Gd-3Y-0.5Zr alloy. Different kinds of refiners were added to the melt attempts to reduce the fraction of inclusions. It is found that the alloys with lower amount of inclusions (with addition of certain refiner) exhibit lower HTS and better fluidity. As a result, reduction of the amount of inclusions might be a solution to achieve better hot tearing resistance.

5.3. Grain size and grain morphology

Both grain size and grain morphology have a great impact on hot tearing behaviour [83–87]. Most of results show that

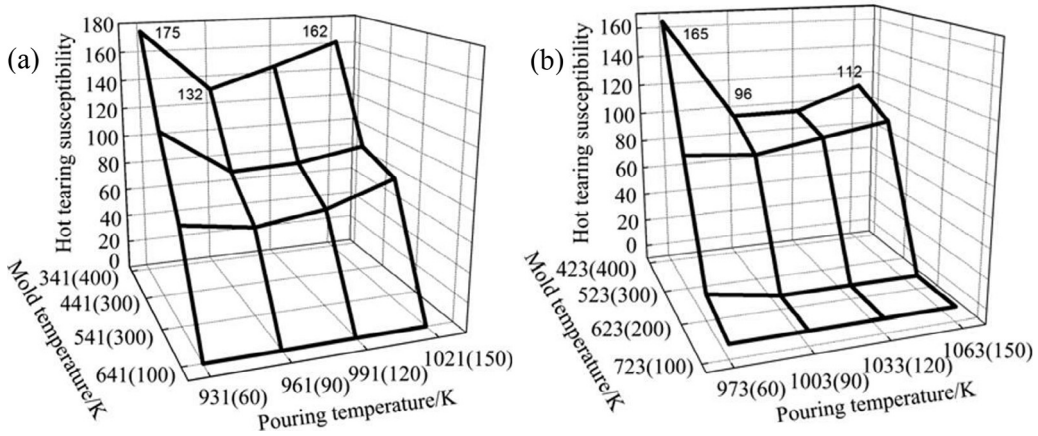

Fig. 17. Influence of pouring temperature and mould temperature on the hot tearing susceptibility of (a) AZ91D and (b) NZ30 [77].

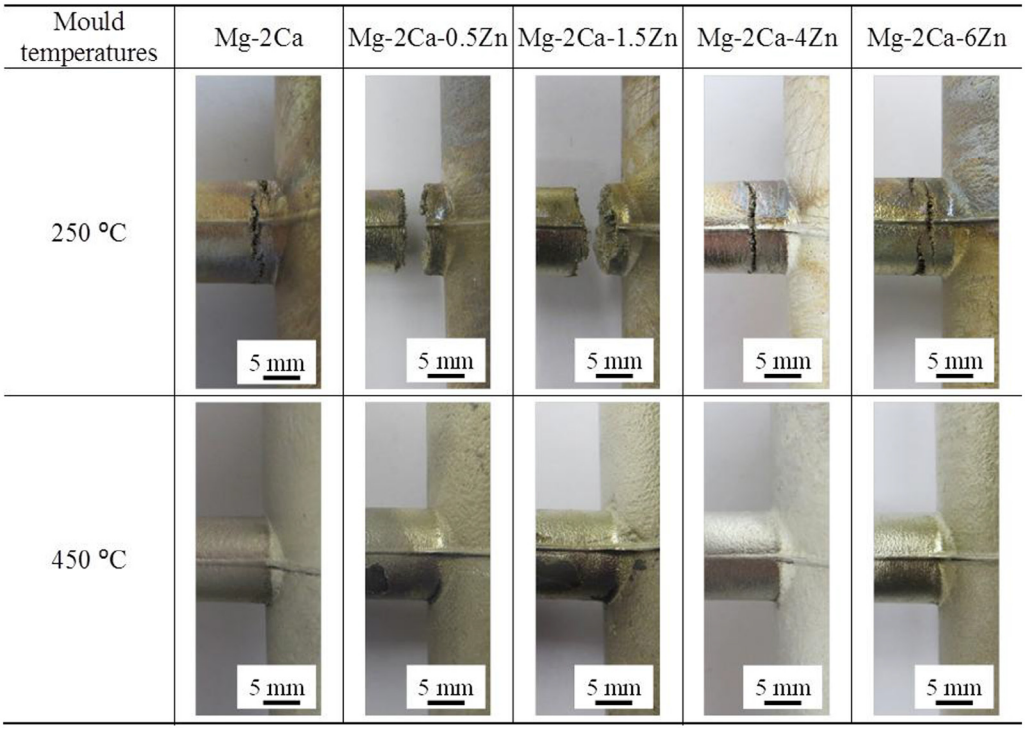

Fig. 18. Macrograph showing the hot tearing susceptibility of Mg-2Ca-Zn alloys at different mould temperatures [79].

grain refinement improves hot tearing resistance, as shown in Wang et al.'s work [36] (Fig. 19). As validated by experiments, the addition of grain refiner decreases the total contraction during solidification [88]. In addition, grain refinement delays the onset of strength development and prolongs mass feeding [84]. The duration of bulk liquid feeding is enhanced for the refined casting conditions and thus, hot tearing severity is reduced [14]. Moreover, this refined grain size is better for the accommodation of deformation caused by the solidification shrinkage. Furthermore, the local strain at the grain boundaries is smaller in the refined alloy than that in the non-refined alloy. Hence the hot tearing tendency is reduced due to the low local strain.

However, it is also predicted with RDG model that the refined grain size would decrease the permeability of the mush, which then increases the HTS [83]. Easton et al.'s modelling suggests that grain refinement reduces the HTS until the grain morphology becomes globular [84]. Further grain refinement causes HTS to increase again. Evidence of increased HTS in grain refined alloy is not experimentally observed. It is commonly acknowledged that columnar and twinned columnar crystals are detrimental to hot tearing, due to the structure promoting easy initiation and propagation of hot cracking [25,55,83].

6. Hot tearing susceptibility of magnesium alloys

6.1. Binary alloys

Hot tearing behaviour of Mg-Al [7,28,54,66,71,89], Mg-Zn [24,71,90], Mg-Ca [26], and Mg-RE [25,37,55,91–93] binary alloys was investigated, as summarized in Table 1. All alloying systems show the maximum cracking tendency at a certain alloy composition. This tendency is known to follow a lambda (Λ) curve.

6.1.1. Mg-Al

Cao et al. [28] investigated the HTS of binary Mg-Al alloys (from 0.25 to 8.0 wt.% Al) using a CRC mould (Fig. 7). The mould temperature was kept constant at 335 °C for all the castings. The HTS of Mg-Al alloys follows the "Λ" shape and the maximum HTS appears at Mg-1 wt.% Al.

Hot tearing tests of binary Mg-Al (1, 3, 6, and 9, wt.%) alloys were also carried out with an instrumented CRC mould (Fig. 10) [66]. The HTS is defined as the crack volume measured from the wax penetration method. It is found that HTS decreases with increasing in Al content. The maximum susceptibility to hot tearing occurs at Mg-1Al alloy, which coincides with Cao et al.'s [28] findings. The effect of different mould temperatures (250 °C, 350 °C, 420 °C, and 500 °C) on the HTS was also studied in their work. The results show that the HTS decreases as mould temperature increases.

6.1.2. Mg-Zn

Investigation on hot tearing behaviour of Mg-Zn alloys has been carried out with an instrumented CRC mould [24,78]. Zn contents ranging from 0.5–12 wt.% were studied in detail with the mould temperature of 200 °C, 300 °C, 450 °C, and 550 °C, respectively. The HTS, denoted by crack volume measured with wax penetration method, decreases with increasing mould temperature. It is also found that the predicted cracking susceptibility coefficient (CSC) with Clyne and Davies's model agrees well with experimental results, as previously shown in Fig. 1.

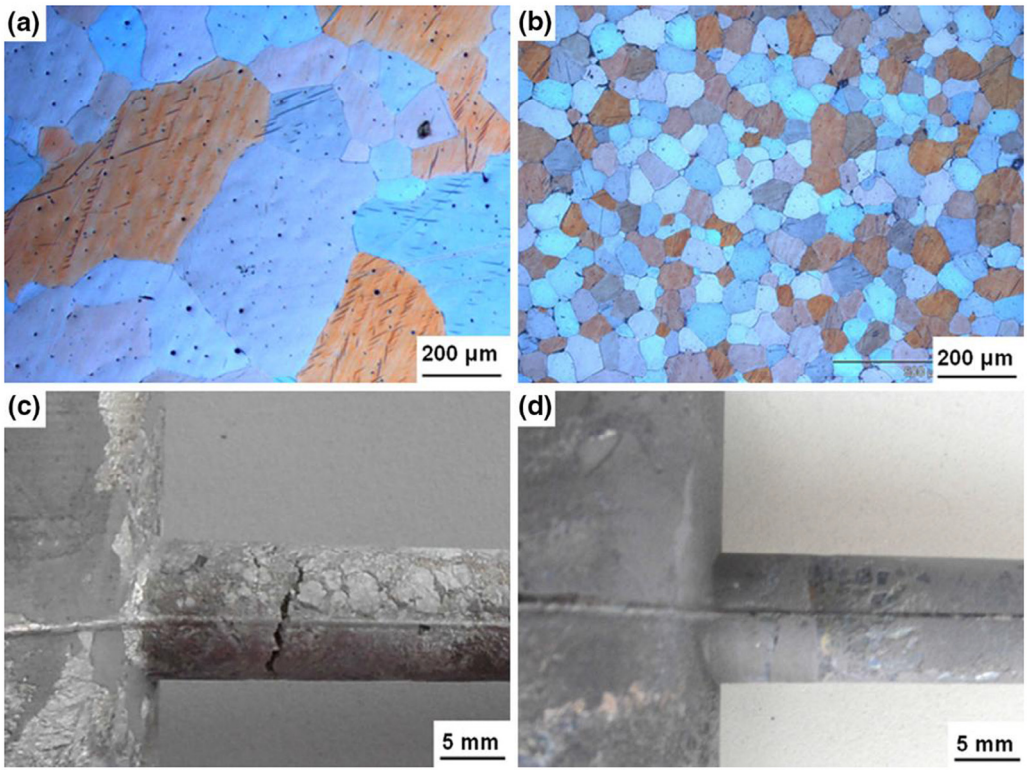

Fig. 19. Optical micrographs (OM) and macro photographs showing the effect of grain size on the HTS of (a), (c) Mg-4.5Zn-0.4Y, (b), (d) Mg-4.5Zn-0.4Y-0.2Zr [36].

Both curves follow the "Λ" shape and the peak of HTS appears at Mg-1.5 wt.% Zn.

6.1.3. Mg-Ca

The same instrumented CRC mould was used to study the hot tearing behaviour of five Mg-Ca (x = 0.1, 0.2, 0.5, 1, and 2, wt.%) alloys. The crack volumes obtained from X-ray tomography technique are shown in Fig. 20 [26]. Mg-0.5Ca and Mg-1Ca were completely broken at a mould temperature of 250 °C, showing the highest HTS among all. As the mould temperature increases to 450 °C, the HTS decreases dramatically.

6.1.4. Mg-RE

Mg-RE alloys are of significant interest for their excellent properties, particularly for high temperature creep resistant and high strength applications. The hot tearing behaviour of Mg-Y, Mg-Gd, Mg-La, Mg-Ce, and Mg-Nd was investigated.

Hot tearing susceptibility of Mg-Y (0.2–4, wt.%) alloys cast at two different mould temperatures was investigated [25,37,94]. The HTS is also defined as the crack volume, which is determined from two methods. The crack volume measured with wax penetration method is larger than that with X-ray micro-tomography method (Fig. 21). Such difference results from the limitation of the wax penetration method, since it is difficult to remove the unwanted wax on the surface completely. However, crack volume measured with both methods shows the similar trend and Mg-0.9Y displays the highest HTS among all. It is explained that the high HTS of Mg-0.9Y is due to its large grain size, large solidification range, and small amount of eutectic. Besides, the increment in mould temperature from

Table 1
Hot tearing susceptibility (HTS) of binary Mg alloys reported in literatures.

Alloys	Investigated compositions (wt.%)	Alloy with peak HTS (wt.%)	Reference
Mg-Al	0.25, 0.6, 1, 2, 4, 8	Mg-1Al	Cao et al. [28]
	1, 3, 6, 9	Mg-1Al	Zhen et al. [66]
Mg-Zn	0.5, 1, 1.5, 2 4, 6, 9, 12	Mg-1.5Zn	Zhou et al. [24,78]
Mg-Ca	0.1, 0.2, 0.5, 1.0, 2.0	Mg-0.5Ca, Mg-1Ca	Song et al. [26]
Mg-Y	0.2, 0.9, 1.5, 2, 4	Mg-0.9Y	Wang et al. [25]
Mg-Gd	1, 2, 5, 10	Mg-2Gd	Srinivasan et al. [55]
Mg-La	0.51, 0.94, 1.71, 3.44, 5.07	Mg-1.71La	Easton et al. [93]
Mg-Ce	0.53, 0.93, 1.48, 2.87, 4.76	Mg-0.53Ce	Easton et al. [93]
Mg-Nd	0.47, 0.76, 0.84, 1.18, 1.25, 1.5, 2.6, 3.53, 6.75, 8.05	Mg-(1.18–6.75)Nd*	Easton et al. [93]

* All the Mg-(1.18–6.75) Nd alloys show high HTS, most alloys are completely broken.

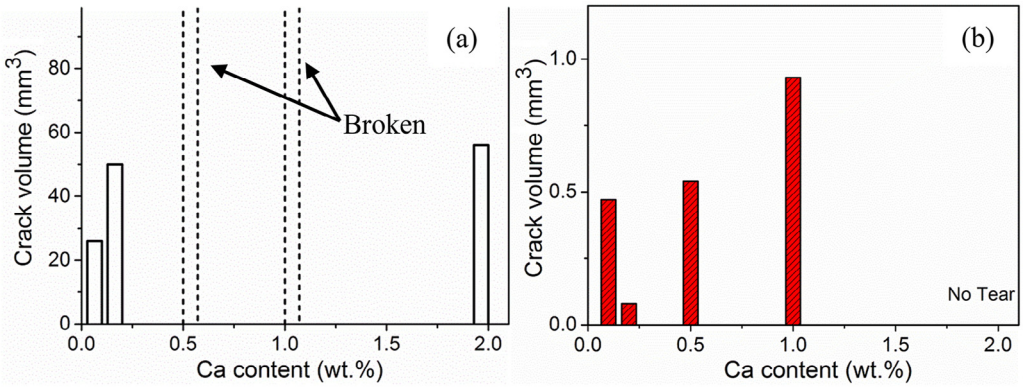

Fig. 20. Crack volumes of Mg-Ca alloys cast at (a) 250 °C and (b) 450 °C [26].

250 °C to 450 °C significantly reduces the HTS of binary Mg-Y alloys.

Srinivasan et al. [55,91] studied the hot tearing characteristics of binary Mg-Gd (1–10, wt.%) alloys with an instrumented CRC mould. Similar to Mg-Y alloys, larger crack volume is obtained with the wax penetration method than X-ray tomography technique. It is found that the susceptibility to hot tearing increases with increase in Gd content, reaches a maximum at 2 wt.% Gd and then decreases with further increment of Gd content, as shown in Fig. 22. The high susceptibility observed in Mg-2 wt.% Gd was attributed to cellular or columnar grain structure, which facilitates the tear propagation. The effect of mould temperature on HTS is similar to that of Mg-Y alloys.

The HTS and phase diagram of binary Mg-La, Mg-Ce, and Mg-Nd alloys are compared in Fig. 23 [93]. It is found that the HTS of the alloy series is related to their FR. Mg-Nd alloy system having the largest FR and highest HTS among all. A further observation is that Mg-Nd alloys have the highest eutectic composition, and hence have the lowest amount of eutectic for a particular alloy composition.

6.2. Ternary alloys

Testing results of HTS of ternary Mg-Al-Zn [47,78], Mg-Al-Ca [51], Mg-Al-Sr [11,52], Mg-Zn-Y [49,74,95], and Mg-Zn-Ca [79,96,97] alloys were reported and summarized in Table 2. The ternary alloys show maximum HTS at a certain composition. However, the HTS sometimes does not follow the "Λ" shape.

6.2.1. Mg-Al-Zn

Wang et al. [47] used a ring mould casting to study the hot tearing behaviour of Mg-9Al-xZn (x range from 0.2 to 1.0 wt.%) alloys. The hot tearing severity is related to the critical diameter of round steel in the centre. It is reported that HTS increases as Zn content within the whole investigated range increases. The inter-crystalline segregation of Zn and Al is thought to be the main contribution to the high HTS of Mg-9Al-xZn alloys.

Hot tearing tests of ternary Mg-Al-Zn alloys were also performed with the instrumented CRC mould at a mould temperature of 200 °C [27]. Mg-0.5Al-xZn (x = 0.5, 1.5, 2.5, and 4, wt.%) alloys, Mg-xAl-1.5Zn (x = 0.5, 3, and 6, wt.%) alloys, and Mg-xAl-4Zn (x = 0.5, 3, and 6, wt.%) alloys were investigated. The effects of Al and Zn content on the HTS of Mg-Al-Zn alloys are shown in Fig. 24. The crack volume measured by wax penetration method is used as the index of HTS. It is revealed that, for Mg-xZn-0.5Al alloys, two peaks of HTS are obtained: one appears at about 1.0 to 1.5 wt.% Zn, the other occurs at about 3.0 wt.%. In both Mg-1.5Zn-xAl and Mg-4Zn-xAl ternary alloy systems, the HTS decreases with increasing Al content.

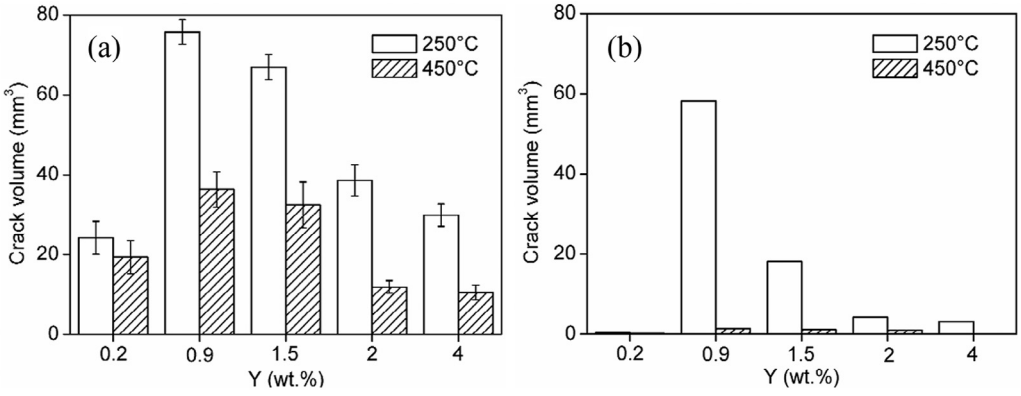

Fig. 21. Crack volumes of Mg-Y alloys measured with (a) wax penetration method and (b) X-ray tomography technique [94].

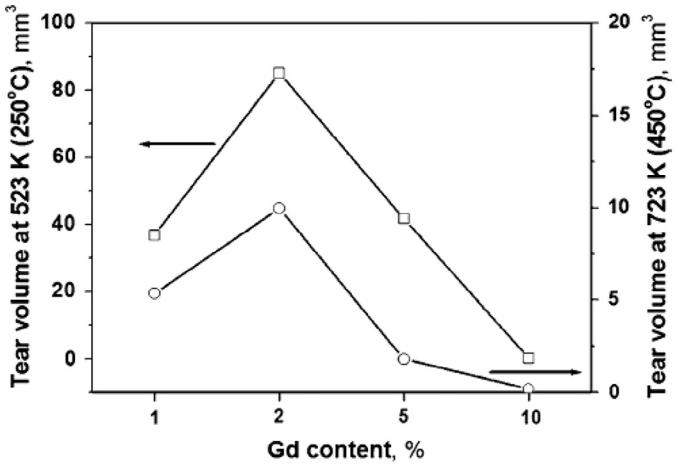

Fig. 22. Tear volume of Mg-Gd alloys measured by X-ray tomography technique [55].

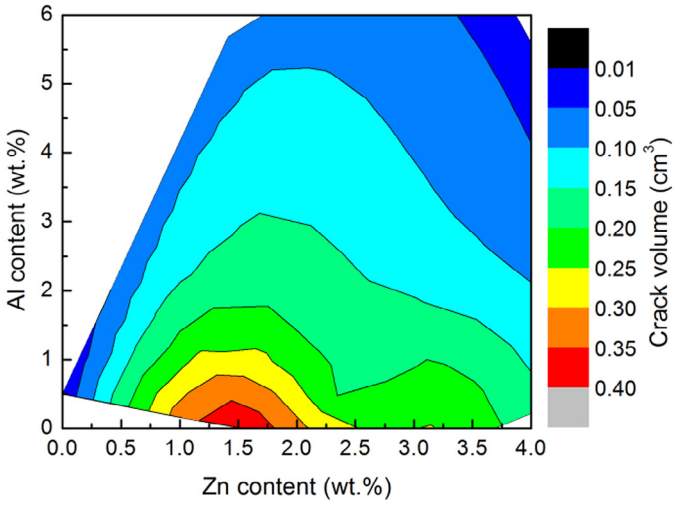

Fig. 24. Crack volume of ternary Mg-Al-Zn alloys, the original data is taken from Ref. [27].

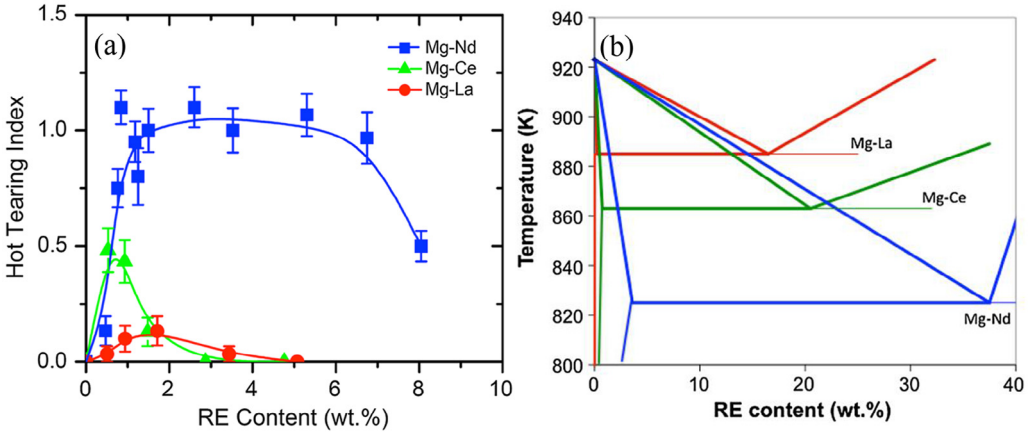

Fig. 23. (a) Hot tearing index of binary Mg-RE alloys, (b) overlayed phase diagrams of Mg-RE alloys assuming straight liquidus and solidus lines [93].

Table 2
Hot tearing susceptibility (HTS) of several ternary Mg alloys.

Alloys	Investigated compositions (wt.%)	Composition with peak HTS (wt.%)	Ref
Mg-9Al-xZn	x = 0.2, 0.4, 0.6, 0.8, 1.0	Mg-9Al-1.0Zn	Wang et al. [47]
Mg-0.5Al-xZn	x = 0.5, 1.5, 2.5, 4	Mg-1.5Zn-0.5Al	Zhou et al. [78]
Mg-xAl-1.5Zn	x = 0.5, 3, 6	Mg-1.5Zn-0.5Al	Zhou et al. [78]
Mg-xAl-4Zn	x = 0.5, 3, 6	Mg-1.5Zn-4Al	Zhou et al. [27]
Mg-4Al-xCa	x = 0.5, 1.5, 2.5, 3.5	Mg-4Al-0.5Ca	Cao et al. [51]
Mg-xAl-2.5Ca	x = 4, 5, 6	Mg-5Al-2.5Ca*	Cao et al. [51]
Mg-xAl-1.5Sr	x = 4, 6, 8	Mg-4Al-1.5Sr	Cao et al. [11,52]
Mg-xAl-3Sr	x = 4, 6, 8	Mg-4Al-3Sr	Cao et al. [11,52]
Mg-4.5Zn-xY	x = 0.4, 0.9, 2	Mg-4.5Zn-0.9Y	Wang et al. [36]
Mg-1.5Zn-xY	x = 0.2, 2, 3	Mg-1.5Zn-0.2Y	Wang et al. [74]
Mg-3Zn-xY-0.5Zr†	x = 0.4, 0.8	Mg-3Zn-0.4Y-0.5Zr	Gunde et al. [49]
Mg-2.5Zn-xY-0.5Zr†	x = 0.5, 1, 2, 4, 6	Mg-2.5Zn-2Y-0.5Zr	Liu et al. [95]
Mg-xZn-0.5Ca	x = 0.5, 1.5, 4, 6	Mg-0.5Ca-4Zn	Song et al. [96]
Mg-xZn-2Ca	x = 0.5, 1.5, 4, 6	Mg-2Ca-0.5Zn	Song et al. [79]
Mg-4Zn-xCa	x = 0.2, 0.5, 1, 2	Mg-0.5Ca-4Zn	Song et al. [97]

* The content of Al has minor effect on the HTS of Mg-xAl-2.5Ca alloys.
† The alloys are shown here as Zr is only used as grain refiner.

6.2.2. Mg-Al-Ca

The hot tearing severity of Mg-Al-Ca alloys was compared with the commercial AZ91E alloy [51], as displayed in Fig. 25. The experiments were carried out with an instrumented CRC mould at a constant mould temperature of 335 °C. The evaluation of HTS takes the width, length and the location of the crack into consideration. Among all the investigated alloys, Mg-4Al-2.5Ca, Mg-4Al-3.5Ca, Mg-5Al-2.5Ca, and Mg-6Al-2.5Ca have either similar or slightly lower susceptibility to hot tearing compared to that commercial alloy AZ91E. AZ91E is known to have a low HTS. The HTS of Mg-4Al-xCa alloys decreases sharply with increasing Ca content. The susceptibility to hot tearing does not change significantly as the Al content increases from 4 to 6 wt.% in Mg-xAl-2.5Ca (x = 4, 5, and 6) alloys.

6.2.3. Mg-Al-Sr

Investigation of HTS of Mg-Al-Sr alloys was carried out with the same mould used in Mg-Al-Ca alloys [11,52]. The mould temperature was also kept at 335 °C and the evaluation method was also the same as described for Mg-Al-Ca alloys. HTS of Mg-xAl-1.5Sr and Mg-xAl-3Sr alloys are also compared with that of AZ91E, as shown in Fig. 26. The results indicate that the HTS of Mg-xAl-1.5Sr is higher than AZ91E and the HTS of Mg-xAl-3Sr is similar to that of AZ91E. HTS decreases with increasing Al content in both Mg-xAl-1.5Sr and Mg-xAl-3Sr alloys.

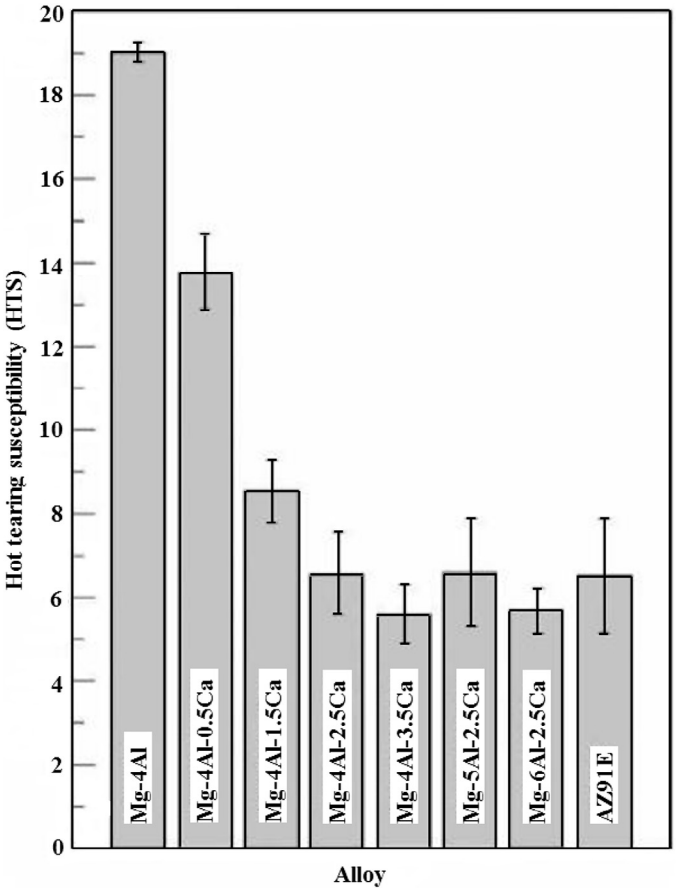

Fig. 25. Hot tearing susceptibility of ternary Mg-Al-Ca alloys and AZ91E evaluated with CRC apparatus [51].

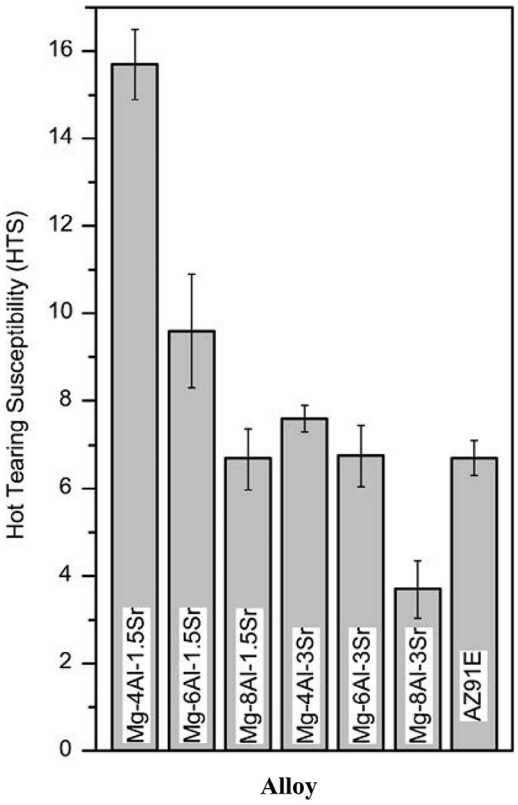

Fig. 26. Hot tearing susceptibility of ternary Mg-Al-Sr alloys and AZ91E evaluated with CRC apparatus [11].

6.2.4. Mg-Zn-Y

The influences of Y addition on the hot tearing behaviour of Mg-1.5Zn and Mg-4.5 Zn alloys were investigated [36,74]. Experiments were carried out using an instrumented CRC apparatus. The Mg-1.5Zn-xY (x = 0.2, 2, and 3, wt.%) alloys were only cast at 250 °C. Two mould temperatures (250 °C and 450 °C) were applied to the hot tearing tests for Mg-4.5Zn-xY (x = 0.4, 0.9, and 2, wt.%) alloys. The crack volume measured with wax penetration method is used as the index of HTS for both alloy systems, as compared in Fig. 27. The HTS of Mg-1.5Zn-xY alloys decreases with increment in Y content. The large grain size and solidification range account for the maximum HTS occurred in Mg-1.5Zn-0.2Y alloy. Mg-4.5Zn-xY alloys exhibit high HTS, as both Mg-4.5Zn-0.4Y and Mg-4.5Zn-0.9Y alloys were completely broken at a mould temperature of 250 °C.

Gunde et al. [49] studied the HTS of Mg-3Zn-0.4Y-0.5Zr and Mg-3Zn-0.8Y-0.5Zr alloys with the permanent star-shaped mould (Fig. 6). As the addition of Zr is mainly for grain refinement, the alloy is classified as Mg-Zn-Y alloys. In their study, both alloys were cast at a mould temperature of 250 °C. The Y content increases from 0.4 wt.% to 0.8 wt.% results in a significant reduction of HTS. The decreased susceptibility is attributed to the reduced terminal freezing range with the addition of Y. The terminal freezing range is defined as the temperature interval at the solid fraction of 0.9 and 0.98.

Hot tearing severity of Mg-2.5Zn-xY-0.5Zr (x = 0.5, 1, 2, 4 and 6, wt.%) alloys was evaluated with an instrumented CRC

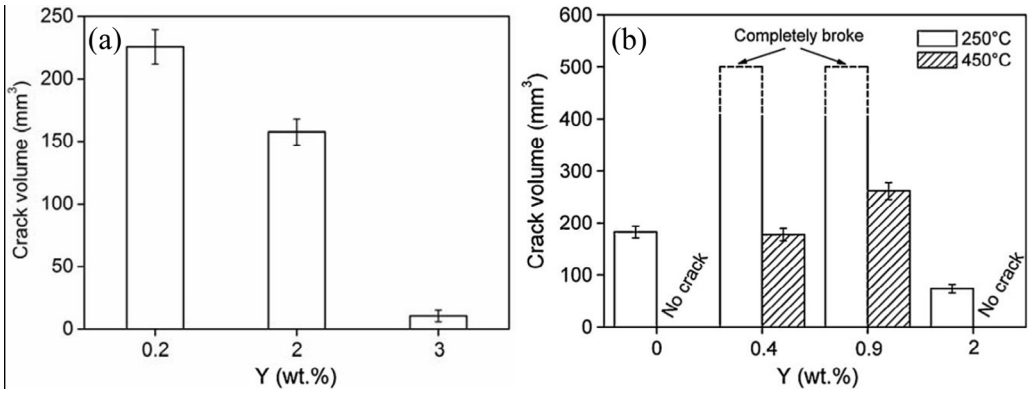

Fig. 27. Crack volumes measured with wax penetration of (a) Mg-1.5Zn-xY alloys cast at 250 °C [74] and (b) Mg-4.5Zn-xY alloys cast at 250 °C and 450 °C [36].

mould [95]. They found that the HTS of Mg-2.5Zn-1Y-0.5Zr alloy is the lowest among all and the HTS of Mg-2.5Zn-2Y-0.5Zr is the highest among all. A good correlation between HTS and solidification temperature is established.

6.2.5. Mg-Zn-Ca

Effects of Zn and Ca content on the HTS of ternary Mg-Zn-Ca alloys were studied [79,96,97]. Mg-xZn-0.5Ca, Mg-xZn-2Ca (x = 0.5, 1.5, 4, and 6, wt.%) and Mg-4Zn-xCa (x = 0.2, 0.5, 1, and 2, wt.%) alloys were cast in an instrumented CRC mould. The hot tearing severity is acquired from the crack volume measured with X-ray tomography technique, as compared in Fig. 28. The results indicate that Mg-Ca-Zn alloys have an extremely high HTS, as most alloys were completely broken. The element Ca plays more significant role in tailoring the HTS of ternary Mg-Ca-Zn alloys than Zn. Higher amount of Ca content reduces the HTS.

6.3. Commercial alloys

Investigation on hot tearing behaviour of commercial Mg alloys was mainly performed on AZ91. For other alloys there are only few data available, which is also reviewed. The HTS of commercial alloys is not always shown with a certain value but is rather represented comparatively, showing the effect of various cast conditions on a certain alloy. The effect of some elements on the HTS of commercial alloys is also reported.

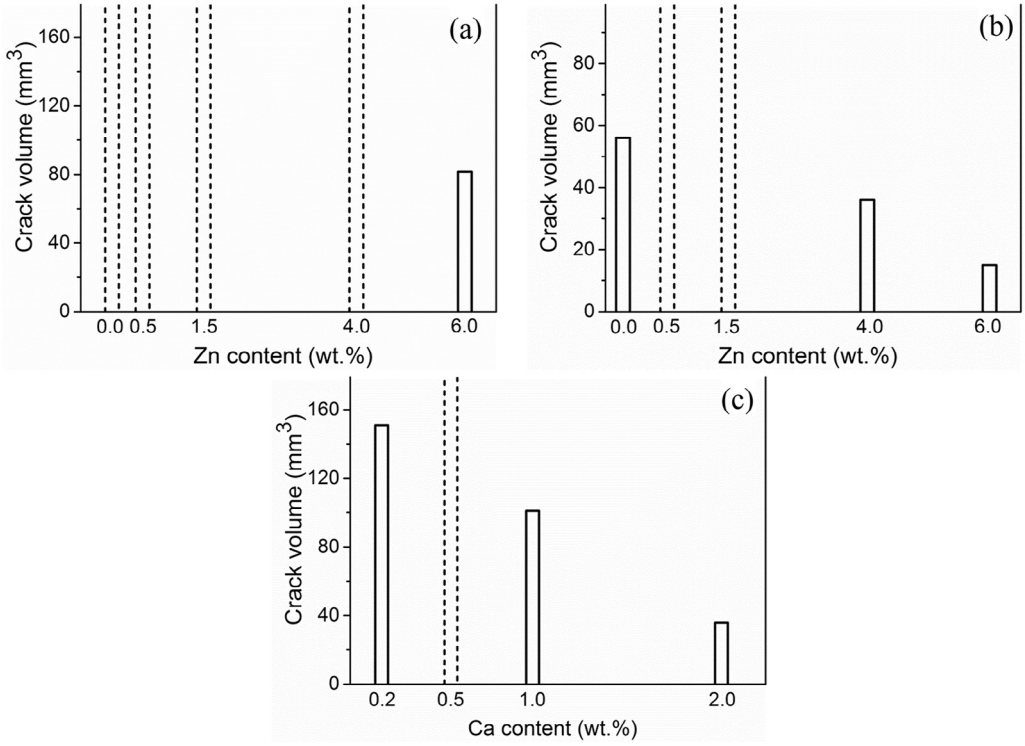

Fig. 28. Crack volumes measured with X-ray tomography of (a) Mg-xZn-0.5Ca alloys [96], (b) Mg-xZn-2Ca alloys [79], and (c) Mg-4Zn-xCa alloys [97] cast at the mould temperature of 250 °C. Dashed column indicates the sample is completely broken.

Table 3
Effects of element on the HTS of commercial alloys.

Base alloys	Adding elements	Adding amount (wt.%)	Influence of the addition on HTS	Reference
AZ91D	Ca	0.1, 0.3, 0.4, 0.6, 0.8, 1.0	HTS increase with increasing Ca content	Li et al. [101]
AZ91D	Ca	0.1, 0.3, 0.5, 0.8, 1.0	HTS increase with increasing Ca content	Tang et al. [99]
AZ91D	0.4Ca + Sr	0.01, 0.05, 0.10, 0.20	Addition of Sr to AZ91D + 0.4 wt.% Ca reduces HTS	Tang et al. [99]
AZ91	Ca	0.5, 1.5, 2.5	Addition of Ca promotes the formation of hot tears	Hort et al. [102]
AZ91	Zn	1, 2, 3, 4, 5, 6, 7	Addition of Zn does not promote hot tearing	Hort et al. [102]
AZ31	RE	0.1, 0.2, 0.5, 0.8, 1.2	HTS increase with increasing RE content	Zheng et al. [100]
AZ91	RE	0.1, 0.2, 0.5, 0.8, 1.2	HTS increase with increasing RE content	Zheng et al. [100]
AM60	RE	0.1, 0.2, 0.5, 0.8, 1.2	HTS increase with increasing RE content	Zheng et al. [100]
AM60B	Sr	0.005, 0.01, 0.02, 0.05, 0.1, 0.2	HTS decreases with increasing Sr content	Li et al. [50]

Hot tearing behaviour of AZ91 was extensively studied using different apparatuses with attempts to clarify its hot tearing mechanism. Wang et al. [98] performed hot tearing test on AZ91 with a ring mould. It is revealed that the hot tearing initiation temperature of AZ91 is the practical temperature at the end of solidification (eutectic temperature). M. Pokorny et al. [89] carried out hot tearing cast of AZ91D in a permanent steel mould to validate their proposed hot tearing model. The prediction with their viscoplastic deformation model agrees well with the hot tearing test of AZ91D. Other researchers attempt to study the effect of pouring temperature and mould temperature on HTS of AZ91 [76,77]. The results suggest that increasing the mould temperature significantly reduces HTS of AZ91. The effect of pouring temperature on HTS is less pronounced than that of varying the mould temperature.

Effect of trace elements on hot tearing behaviour of commercial alloys was also studied [50,99–102], as summarized in Table 3. Li et al. [101] studied the influence of Ca addition (0–1 wt.%) on the hot tearing behaviour of AZ91D. It is found that the HTS of AZ91D increases with increase in Ca content. The effects of Ca and Sr composite addition into AZ91D alloy on the hot cracking resistance were investigated by Tang et al. [99]. The addition of Ca decreases the hot cracking resistance of AZ91D alloys. Adding Sr to Ca-containing AZ91D alloy effectively improved its hot tearing resistance. Zn and Ca were also added to AZ91 by Hort et al. [102]. The addition of both Zn and Ca results in incomplete filling at low mould temperatures below 350 °C. The addition of Ca induced hot tears. The base alloy AZ91 and alloys with addition of Zn show no visible crack. The effect of Ca content on the HTS of AZ91 is not given in detail in their study.

Effect of RE on hot cracking behaviour of AZ31, AZ91, and AM60 was also studied [100]. Results show that the addition of RE increases the HTS of these commercial alloys. Among these three commercial alloys, AZ91 shows the lowest susceptibility to hot tearing. Li et al. [50] investigated the influence of Sr on HTS of AM60B. Only a small amount of Sr addition (0.005 wt.%) is capable of improving the hot tearing resistance of AM60B. The hot tearing behaviour of sand cast WE54 alloys with and without Zr addition was studied [87]. It is stated that the addition of Zr to WE 54 alloy delays the onset of hot tearing and finally decreases the HTS.

The HTS of several alloys were compared in Table 4 [103]. Among them, the highest HTS is observed in the AE42 alloy and the lowest is found in AJ62x and AJ62Lx alloys. HTS of several AXJ alloys was evaluated in thin wall die casting and compared with that of AM50 [104]. In general, the HTS increases with the addition of Ca and Sr to AM50. The addition of Ca increased the frequency and severity of hot cracking but raising the Ca level to 1.7% (AXJ520) improved the casting rating, although not to the level of AM50. With even higher Ca additions, the hot cracking deteriorated again.

7. Conclusion

In this review, hot tearing criteria, experimental apparatuses and the hot tearing susceptibility of magnesium alloys are summarized. The basic physics of hot tearing phenomenon has been established and understood. However, each existing criterion still has its own limitations to predict and/or simulate the initiation and propagation of hot tearing. Thus, a reliable hot tearing criterion that is capable of accurately predicting the hot tearing behaviour under various conditions of all alloy systems is still required, and the numerical simulation should also focus on a more precise hot tearing model. Various apparatuses have been designed and developed to study the hot tearing behaviour of Mg alloys. However, a standard hot tearing test system and a standard evaluation method of hot tearing severity need to be established and developed. In order to acquire comparable hot tearing susceptibility of alloys, a consistent approach should be

Table 4
Hot tearing ratings of various Mg alloys. Data is provided in Ref. [103]. Higher rating indicates higher HTS.

Alloy	Average hot tearing rating
AZ91D	20
AZ91E	14
AM50A	44
ITM*	61
AJ50x	45–60
AS21	69
AS21x	27
AS41B	82
AE42	94
AJ51x	35–50
AJ52x	24
AJ53x	5
AJ62x	0
AJ62Lx	0

* ITM (AX51, 0.8% Ca).

agreed upon. Besides, technique/apparatus that can *in situ* observe on the formation and propagation of hot tearing in Mg alloys is to be developed. Hot tearing studies on several Mg alloys indicate that their hot tearing susceptibility relies on its composition, casting parameters and microstructures.

Acknowledgements

The present work was supported by the National Natural Science Foundation of China (Project 51531002, 51474043), the Ministry of Science & Technology of China (2013DFA71070), the Ministry of Education of China (SRFDR 20130191110018) and Chongqing Municipal Government (CSTC2013JCYJC60001, CEC project, Two River Scholar Project and The Chief Scientist Studio Project).

References

[1] A. Luo, JOM 54 (2002) 42–48.
[2] K.U. Kainer, Magnesium Alloys and Technology, Wiley-VCH GmbH, Germany, 2003.
[3] H.E. Friedrich, B.L. Mordike, Magnesium Technology, Springer Berlin Heidelberg, Germany, 2006.
[4] A. Luo, J. Magnes. Alloys 1 (2013) 2–22.
[5] L. Katgerman, D.G. Eskin, Hot Cracking Phenomena in Welds II, Springer Berlin Heidelberg, Berlin, 2008, pp. 11–26.
[6] Z. Shi, W.J. Kim, F. Cao, M.S. Dargusch, A. Atrens, J. Magnes. Alloys 3 (2015) 271–282.
[7] Z.S. Zhen, N. Hort, Y. Huang, O. Utke, N. Petri, K.U. Kainer, Int. J. Cast Metal Res. 22 (2009) 331–334.
[8] A.K. Dahle, D.H. StJohn, Acta Mater. 47 (1998) 31–41.
[9] D.G. Eskin, Suyitno, L. Katgerman, Prog. Mater. Sci. 49 (2004) 629–711.
[10] M. M'Hamdi, A. Mo, H. Fjær, Metall. Mater. Trans. A 37 (2006) 3069–3083.
[11] G. Cao, C. Zhang, H. Cao, Y.A. Chang, S. Kou, Metall. Mater. Trans. A 41 (2010) 706–716.
[12] D.G. Eskin, L. Katgerman, Metall. Mater. Trans. A 38 (2007) 1511–1519.
[13] D.J. Lahaie, M. Bouchard, Metall. Mater. Trans. B 32 (2001) 697–705.
[14] F. D'Elia, C. Ravindran, D. Sediako, Mater. Sci. Eng. A 624 (2015) 169–180.
[15] B. Magnin, L. Maenner, L. Katgerman, S. Engler, Mater. Sci. Forum 217–222 (1996) 1209–1214.
[16] M. Rappaz, J.M. Drezet, M. Gremaud, Metall. Mater. Trans. A 30 (1999) 449–455.
[17] M. Bellet, G. Qiu, J. Carpreau, J. Mater. Process. Tech. 230 (2016) 143–152.
[18] Suyitno, W.H. Kool, L. Katgerman, Metall. Mater. Trans. A 36 (2005) 1537–1546.
[19] M. Braccini, C.L. Martin, M. Suery, Y. Brechet, Modeling of Casting, Welding and Advanced Solidification Processes IX, Shaker Verlag GmbH, Aachen, Germany, 2000, pp. 18–24.
[20] J.F. Grandfield, C.J. Davidson, J.A. Taylor, Light Metals 2001 (2001) 895–901.
[21] T.W. Clyne, G.J. Davies, Solidification and Casting of Metals, Metals Society, London, 1979, pp. 275–278.
[22] T.W. Clyne, G.J. Davies, Brit. Foundryman 74 (1981) 65–73.
[23] T.W. Clyne, G.J. Davies, Brit. Foundryman 68 (1975) 238–244.
[24] L. Zhou, Y.D. Huang, P.L. Mao, K.U. Kainer, Z. Liu, N. Hort, Int. J. Cast Metal Res. 24 (2011) 170–176.
[25] Z. Wang, Y. Huang, A. Srinivasan, Z. Liu, F. Beckmann, K.U. Kainer, et al., Mater Design 47 (2013) 90–100.
[26] J. Song, Z. Wang, Y. Huang, A. Srinivasan, F. Beckmann, K.U. Kainer, et al., Metall. Mater. Trans. A 46A (2015) 6003–6017.
[27] L. Zhou, School of materials science and engineering (Doctoral thesis), Shenyang University of Technology, China, 2011. (in Chinese).
[28] G. Cao, S. Kou, Mater. Sci. Eng. A 417 (2006) 230–238.
[29] Suyitno, W.H. Kool, L. Katgerman, Mater. Sci. Forum 396–402 (2002) 179–184.
[30] S. Kou, Acta Mater. 88 (2015) 366–374.
[31] J. Liu, S. Kou, Acta Mater. 100 (2015) 359–368.
[32] J. Liu, S. Kou, Acta Mater. 110 (2016) 84–94.
[33] E.W. Postek, R.W. Lewis, D.T. Gethin, Int. J. Numer. Meth. Heat Fluid Flow 18 (2008) 325–355.
[34] N. Hatami, R. Babaei, M. Dadashzadeh, P. Davami, J. Mater. Process. Tech. 205 (2008) 506–513.
[35] J.Z. Zhu, J. Guo, M.T. Samonds, Int. J. Numer. Meth. Eng. 87 (2011) 289–308.
[36] Z. Wang, J. Song, Y. Huang, A. Srinivasan, Z. Liu, K. Kainer, et al., Metall. Mater. Trans. A 46 (2015) 2108–2118.
[37] Z. Wang, Y. Huang, A. Srinivasan, Z. Liu, F. Beckmann, K. Kainer, et al., J. Mater. Sci. 49 (2014) 353–362.
[38] M. Pokorny, C. Monroe, C. Beckermann, L. Bichler, C. Ravindran, Int. J. Metalcast 2 (2008) 41–53.
[39] C.A. Monroe, C. Beckermann, J. Klinkhammer, Modeling of Casting, Welding, and Advanced Solidification Process-XII, TMS 2009, pp. 313–320.
[40] ESI Group Inc. ProCAST 2030.0 User Manual. 2013.
[41] M. Sistaninia, S. Terzi, A.B. Phillion, J.M. Drezet, M. Rappaz, Acta Mater. 61 (2013) 3831–3841.
[42] M. Sistaninia, A.B. Phillion, J.M. Drezet, M. Rappaz, Acta Mater. 60 (2012) 6793–6803.
[43] A.R.E. Singer, P.H. Jennings, J. I. Met. 73 (1946) 273–284.
[44] P.H. Jennings, A.R.E. Singer, W.I. Pumphrey, J. I. Met. 74 (1948) 227–246.
[45] D. Warrington, D.G. McCartney, Cast Metals 3 (1991) 202–208.
[46] J.M. Drezet, M. Rappaz, Modeling of Casting, Welding, and Advanced Solidification Process VIII, San Antonio, Texas, USA, 1998, pp. 883–890.
[47] Y. Wang, B. Sun, Q. Wang, Y. Zhu, W. Ding, Mater. Lett. 57 (2002) 929–934.
[48] D. Viano, School of mechanical and mining engineering (Doctoral thesis), University of Queensland, Australia, 2011.
[49] P. Gunde, A. Schiffl, P.J. Uggowitzer, Mater. Sci. Eng. A 527 (2010) 7074–7079.
[50] S. Li, B. Tang, X. Jin, D. Zeng, J. Mater. Sci. 47 (2012) 2000–2004.
[51] G. Cao, S. Kou, Metall. Mater. Trans. A 37 (2006) 3647–3663.
[52] G. Cao, I. Haygood, S. Kou, Metall. Mater. Trans. A 41 (2010) 2139–2150.
[53] Z. Zhen, O. Utke, W. Punessen, N. Hort, K.U. Kainer, Patent No. EP 2 187 196 A2, E. Patentanmeldung (.), Germany, 2008. (in German).
[54] Z. Zhen, N. Hort, Y. Huang, N. Petri, O. Utke, K.U. Kainer, Mater. Sci. Forum 618–619 (2009) 533–540.
[55] A. Srinivasan, Z. Wang, Y. Huang, F. Beckmann, K. Kainer, N. Hort, Metall. Mater. Trans. A 44 (2013) 2285–2298.
[56] S. Li, Worcester Polytechnic Institute (Doctoral thesis), America, 2010.
[57] S. Li, D. Apelian, K. Sadayappan, Trans. Am. Foundry Soc. 120 (2012) 149–155.
[58] I. Farup, J.M. Drezet, M. Rappaz, Acta Mater. 49 (2001) 1261–1269.
[59] C. Davidson, D. Viano, L. Lu, D. StJohn, Int. J. Cast Metal Res. 19 (2006) 59–65.
[60] P.D. Grasso, J.M. Drezet, I. Farup, M. Rappaz, Proc Euromat 5263 (2001) 533–544.
[61] A.B. Phillion, R.W. Hamilton, D. Fuloria, A.C.L. Leung, P. Rockett, T. Connolley, et al., Acta Mater. 59 (2011) 1436–1444.
[62] S. Terzi, L. Salvo, M. Suéry, N. Limodin, J. Adrien, E. Maire, et al., Scripta Mater. 61 (2009) 449–452.
[63] A.B. Phillion, S.L. Cockcroft, P.D. Lee, Scripta Mater. 55 (2006) 489–492.
[64] C. Puncreobutr, P.D. Lee, K.M. Kareh, T. Connolley, J.L. Fife, A.B. Phillion, Acta Mater. 68 (2014) 42–51.

[65] K. Hu, A.B. Phillion, D.M. Maijer, S.L. Cockcroft, Scripta Mater. 60 (2009) 427–430.
[66] Z. Zhen, N. Hort, O. Utke, Y. Huang, N. Petri, K.U. Kainer, Magnesium Technology 2009, TMS Wiley, 2009, pp. 105–110.
[67] L. Katgerman, JOM 34 (1982) 46–49.
[68] Suyitno, D.G. Eskin, V.I. Savran, L. Katgerman, Metall. Mater. Trans. A 35 (2004) 3551–3561.
[69] J. Campbell, Casting, Second ed., Elsevier Science Ltd., Great Britain, 2003.
[70] W.S. Pellini, Foundry 80 (1952) 125–199.
[71] Y. Huang, Z. Wang, A. Srinivasan, K.U. Kainer, N. Hort, Acta Phys. Pol. A 122 (2012) 497–500.
[72] Suyitno, D.G. Eskin, L. Katgerman, Metall. Mater. Trans. A 420 (2006) 1–7.
[73] M.A. Easton, H. Wang, J. Grandfield, C.J. Davidson, D.H. StJohn, L.D. Sweet, et al., Metall. Mater. Trans. A 43 (2012) 3227–3238.
[74] Z. Wang, Y.D. Huang, A. Srinivasan, Z. Liu, K.U. Kainer, N. Hort, Mater. Sci. Forum 765 (2013) 306–310.
[75] D.G. Eskin, V.I. Savran, L. Katgerman, Metall. Mater. Trans. A 36 (2005) 1965–1976.
[76] L. Bichler, A. Elsayed, K. Lee, C. Ravindran, Int. J. Metalcast 2 (2008) 43–56.
[77] H. Huang, P. Fu, Y. Wang, L. Peng, H. Jiang, Trans. Nonferr. Metals Soc. 24 (2014) 922–929.
[78] L. Zhou, Y. Huang, P.L. Mao, K.U. Kainer, Z. Liu, N. Hort, Magnesium Technology 2011, John Wiley & Sons, 2011, pp. 125–130.
[79] J. Song, Z. Wang, Y. Huang, A. Srinivasan, F. Beckmann, K.U. Kainer, et al., J. Mater. Sci. 51 (2016) 2687–2704.
[80] G. Wu, J. Dai, M. Sun, W. Ding, Trans. Nonferr. Metals Soc. 20 (2010) 2037–2045.
[81] Y. Huang, School of materials science and engineering (Master thesis), Shanghaijiaotong University, China, 2009. (in Chinese).
[82] G. Wu, M. Sun, W. Wang, W. Din, Trans. Nonferr. Metals Soc. 20 (2010) 1021–1031 (in Chinese).
[83] M. Easton, H. Wang, J. Grandfield, D. StJohn, E. Sweet, Mater. Forum 28 (2004) 224–229.
[84] M. Easton, J. Grandfield, D. StJohn, B. Rinderer, Mater. Sci. Forum 519–521 (2006) 1675–1680.
[85] D. Viano, D. StJohn, J. Grandfield, C. Cáceres, Light Metals 2005, TMS, California, 2005, pp. 895–899.
[86] F. D'Elia, C. Ravindran, D. Sediako, K.U. Kainer, N. Hort, Mater Design 64 (2014) 44–55.
[87] J. Li, R. Chen, Y. Ma, W. Ke, Acta Metall. Sin. 26 (2013) 728–734.
[88] D.G. Eskin, Suyitno, J.F. Mooney, L. Katgerman, Metall. Mater. Trans. A 35 (2004) 1325–1335.
[89] M.G. Pokorny, Prediction of hot tear formation for binary magnesium-aluminium alloys in a permanent mold (Master thesis), University of Iowa, America, 2009.
[90] W. Gan, Y. Huang, Z. Wang, N. Hort, M. Hofmann, Mater. Sci. Forum 768–769 (2014) 428–432.
[91] A. Srinivasan, Z. Wang, Y. Huang, F. Beckmann, K.U. Kainer, N. Hort, Trans. Indian Inst. Metals 65 (2012) 701–706.
[92] Z. Wang, Y. Huang, A. Srinivasan, Z. Liu, K.U. Kainer, N. Hort, Developments in Mechanical Engineering, Stralsund, Germany, 2012, pp. 191–197.
[93] M.A. Easton, M.A. Gibson, S.M. Zhu, T.B. Abbott, Metall. Mater. Trans. A 45 (2014) 3586–3595.
[94] Z. Wang, The faculty of natural and materials science (Doctoral thesis), Clausthal University of Technology, Germany, 2014.
[95] Z. Liu, S. Zhang, P. Mao, F. Wang, Trans. Nonferr. Metals Soc. 24 (2014) 907–914.
[96] J. Song, Z. Wang, Y. Huang, A. Srinivasan, F. Beckmann, K.U. Kainer, et al., Mater Design 87 (2015) 157–170.
[97] J. Song, Z. Wang, Y. Huang, K.U. Kainer, N. Hort, The 10th International Conference on Magnesium Alloys and Their Applications, in: Jeju, Korea, 2015, pp. 825–834.
[98] Y. Wang, B. Sun, Q.G. Wang, Y. Zhu, W. Ding, Mater. Lett. 53 (2002) 35–39.
[99] B. Tang, S. Li, X. Wang, D. Zeng, R. Wu, Scripta Mater. 53 (2005) 1077–1082.
[100] W. Zheng, S. Li, B. Tang, D. Zeng, X. Guo, J. Rare Earth 24 (2006) 346–351.
[101] P. Li, B. Tang, E.G. Kandalova, Mater. Lett. 59 (2005) 671–675.
[102] N. Hort, H. Dieringa, K.U. Kainer, Trans. Indian Inst. Metals 58 (2005) 703–708.
[103] M. Pekguleryuz, P. Labelle, D. Argo, E. Baril, Magnesium Technology 2003, TMS, 2003, pp. 201–206.
[104] B.R. Powell, A.A. Luo, B.L. Tiwari, V. Rezhets, Magnes. Tech. 2002 (2002) 123–129.